Comprehensive 10-Year Strategy for Cancer Control from the Ministry of Health and Welfare of Japan.

References

1. Arbuck SG (1995) Paclitaxel: current developmental approaches of the National Cancer Institute. Semin Oncol 22:55–56
2. Britten CD, Izbicka E, Hilsenbeck S, Lawrence R, Davidson K, Cerna C, Gomez L, Rowinsky EK, Weitman S, Van Hoff DD (1999) Activity of the multitargeted antifolate MTA in the human tumor cloning assay. Cancer Chemother Pharmacol 44:105–110
3. Calvert AH, Walling JM (1998) Clinical studies with MTA. Br J Cancer 78 [Suppl 3]:35–40
4. Celio L, Buzzoni R, Longarini R, Marchiano A, Bajetta E (2002) Pemetrexed in gastric cancer: clinical experience and future perspectives. Semin Oncol 29 [Suppl 18]:63–68
5. Chen VJ, Bewley JR, Smith PG, Andis SL, Schultz RM, Iversen PW, Tonkinson JL, Shih C (2000) An assessment of the antithymine and antipurine characteristics of MTA (LY231514) in CCRF-CEM cells. Adv Enzyme Regul 40:143–154
6. Donehower RC, Rowinsky EK (1993) An overview of experience with taxol (paclitaxel) in the USA. Cancer Treat Rev 19 [Suppl C]:63–78
7. Habeck LL, Mendelsohn LG, Shih C, Taylor EC, Colman PD, Gossett LS, Leitner TA, Schultz RM, Andis SL, Moran RG (1995) Substrate specificity of mammalian folypolyglutamate synthetase for 5,10-dideazatetrahydrofolate analogs. Mol Pharmacol 48:326–333
8. Haller DG (2002) Future directions in the treatment of pancreatic cancer. Semin Oncol 29 [Suppl 20]:31–39
9. Hanauske AR, Chen V, Paoletti P, Niyikiza C (2001) Pemetrexed disodium: a novel antifolate clinically active against multiple solid tumors. Oncologist 6:363–373
10. Hochster H (2002) The role of pemetrexed in the treatment of colorectal cancer. Semin Oncol 29 [6 Suppl 18]:54–56
11. Kano Y, Ohnuma T, Okano T, Holland JF (1988) Effects of vincristine in combination with methotrexate and other antitumor agents in human acute lymphoblastic leukemia cells in culture. Cancer Res 48:351–356
12. Kano Y, Sakamoto S, Kasahara T, Akutsu M, Inoue Y, Miura Y (1991) In vitro effects of amsacrine in combination with other anticancer agents. Leuk Res 15:1059–1064
13. Kano Y, Akutsu M, Tsunoda S, Ando J, Matsui J, Suzuki K, Ikeda T, Inoue Y, Adachi K (1996) Schedule-dependent interaction between paclitaxel and 5-fluorouracil in human carcinoma cell lines in vitro. Br J Cancer 74:704–710
14. Kano Y, Akutsu M, Tsunoda S, Suzuki K, Adachi K (1998) In vitro schedule-dependent interaction between paclitaxel and SN-38 (the active metabolite of irinotecan) in human carcinoma cell lines. Cancer Chemother Pharmacol 42:91–98
15. Kano Y, Akutsu M, Tsunoda S, Furuta M, Yazawa Y, Ando J (1998) Schedule-dependent synergism and antagonism between paclitaxel and methotrexate in human carcinoma cell lines. Oncol Res 10:347–354
16. Kano Y, Akutsu M, Tsunoda S, Mano H, Sato Y, Honma Y, Furukawa Y (2001) In vitro cytotoxic effects of a tyrosine kinase inhibitor STI571 in combination with commonly used antileukemic agents. Blood 97:1999–2007
17. Lieu CH, Chang YN, Lai YK (1997) Dual cytotoxic mechanisms of submicromolar taxol on human leukemia HL-60 cells. Biochem Pharmacol 53:1587–1596
18. McDonald AC, Vasey PA, Adams L, Walling J, Woodworth JR, Abrahams T, McCarthy S, Bailey NP, Siddiqui N, Lind MJ, Calvert AH, Twelves CJ, Cassidy J, Kaye SB (1998) A phase I and pharmacokinetic study of LY231514, the multitargeted antifolate. Clin Cancer Res 4:605–610
19. O'Shaughnessy JA, Gennari A, Conte P (2002) Pemetrexed: a promising new treatment for breast cancer. Semin Oncol 29 [2 Suppl 5]:36–41
20. Paz-Ares L, Ciruelos E, Garcia-Carbonero R, Castellano D, Lopez-Martin A, Cortes-Funes H (2002) Pemetrexed in bladder, head and neck, and cervical cancers. Semin Oncol 29 [Suppl 18]:69–75
21. Paz-Ares L, Bezares S, Tabernero JM, Castellanos D, Cortes-Funes H (2003) Review of a promising new agent—pemetrexed disodium. Cancer [Suppl] 97:2056–2063
22. Raymond E, Louvet C, Tournigand C, Coudray AM, Faivre S, De Gramont A, Gespach C (2002) Pemetrexed disodium combined with oxaliplatin, SN38, or 5-fluorouracil, based on the quantitation of drug interactions in human HT29 colon cancer cells. Int J Oncol 21:361–367
23. Rinaldi DA (1999) Overview of phase I trials of multitargeted antifolate (MTA, LY231514). Semin Oncol 26 [Suppl 6]:82–88
24. Rinaldi DA, Burris HA, Dorr FA, Woodworth JR, Kuhn JG, Eckardt JR, Rodriguez G, Corso SW, Fields SM, Langley C, Clark G, Faries D, Lu P, Van Hoff DD (1995) Initial phase I evaluation of the novel thymidylate synthase inhibitor, LY231514, using the modified continual reassessment method for dose escalation. J Clin Oncol 13:2842–2850
25. Rinaldi DA, Kuhn JG, Burris HA, Dorr FA, Rodriguez G, Eckhardt SG, Jones S, Woodworth JR, Baker S (1999) A phase I evaluation of multitargeted antifolate (MTA, LY231514), administered every 21 days, utilizing the modified continual reassessment method for dose escalation. Cancer Chemother Pharmacol 44:372–380
26. Scagliotti GV, Shin DM, Kindler HL, Vasconcelles MJ, Keppler U, Manegold C, Burris H, Gatzemeier U, Blatter J, Symanowski JT, Rusthoven JJ (2003) Phase II study of pemetrexed with and without folic acid and vitamin B_{12} as front-line therapy in malignant pleural mesothelioma. J Clin Oncol 21:1556–1561
27. Schiff PB, Fant J, Horwitz SB (1979) Promotion of microtubule assembly in vitro by taxol. Nature 277:665–667
28. Schultz RM, Dempsey JA, Kraus LA, Schmid SM, Calvete JA, Laws AL (1999) In vitro sequence dependence for the multitargeted antifolate (MTA, LY231514) combined with other anticancer agents. Eur J Cancer 35 [Suppl 4]:S194
29. Shih C, Thornton DE (1998) Preclinical pharmacology studies and the clinical development of a novel multitargeted antifolate, MTA (LY231514). In: Jackman AL (ed) Anticancer drug development guide: antifolate drugs in cancer therapy. Humana, Totowa, p 183
30. Shih C, Chen VJ, Gossett LS, Gates SB, MacKellar WC, Habeck LL, Shackelford KA, Mendelsohn LG, Soose DJ, Patel VF, Andis SL, Bewley JR, Rayl EA, Moroson BA, Beardsley GP, Kohler W, Ratnam M, Schultz RM (1997) LY231514, a pyrrolo[2,3-d]pyrimidine-based antifolate that inhibits multiple folate-requiring enzymes. Cancer Res 57:1116–1123
31. Shih C, Habeck LL, Mendelsohn LG, Chen VJ, Schultz RM (1998) Multiple folate enzyme inhibition: mechanism of a novel pyrrolopyrimidine-based antifolate LY231514 (MTA). Adv Enzyme Regul 38:135–152
32. Steel GG, Peckham MJ (1979) Exploitable mechanisms in combined radiotherapy–chemotherapy: the concept of additivity. Int J Radiat Oncol Biol Phys 5:85–91
33. Taylor EC, Kuhnt D, Shih C, Rinzel SM, Grindey GB, Barredo J, Jannatipour M, Moran RG (1992) A dideazatetrahydrofolate analogue lacking a chiral center at C-6, N-[4-[2-(2-amino-3,4-dihydro-4-oxo-7H-pyrrolo[2,3-d]pyrimidin-5-yl)ethyl]benzoyl]-L-glutamic acid, is an inhibitor of thymidylate synthase. J Med Chem 35:4450–4454
34. Teicher BA, Alvarez E, Liu P, Lu K, Menon K, Dempsey J, Schultz RM (1999) MTA (LY231514) in combination treatment regimens using human tumor xenografts and the EMT-6 murine mammary carcinoma. Semin Oncol 28:55–62
35. Teicher BA, Chen V, Shih C, Menon K, Forler PA, Phares VG, Amsrud T (2000) Treatment regimens including the multitargeted antifolate LY231514 in human tumor xenografts. Clin Cancer Res 6:1016–1023

36. Tesei A, Ricotti L, De Paola F, Amadori D, Frassineti GL, Zoli W (2002) In vitro schedule-dependent interactions between the multitargeted antifolate LY231514 and gemcitabine in human colon adenocarcinoma cell lines. Clin Cancer Res 8:233–239

37. Tomek S, Emri S, Krejcy K, Manegold C (2003) Chemotherapy for malignant pleural mesothelioma: past results and recent developments. Br J Cancer 88:167–174

38. Tonkinson JL, Marder P, Andis SL, Schultz RM, Gossett LS, Shih C, Mendelsohn LG (1997) Cell cycle effects of antifolate antimetabolites: implications for cytotoxicity and cytostasis. Cancer Chemother Pharmacol 39:521–531

39. Vogelzang NJ, Rusthoven JJ, Symanowski J, Denham C, Kaukel E, Ruffie P, Gatzemeier U, Boyer M, Emri S, Manegold C, Niyikiza C, Paoletti P (2003) Phase III study of pemetrexed in combination with cisplatin versus cisplatin alone in patients with malignant pleural mesothelioma. J Clin Oncol 21:2636–2644

Research Paper

The Tyr-Kinase Inhibitor AG879, That Blocks the ETK-PAK1 Interaction, Suppresses the RAS-Induced PAK1 Activation and Malignant Transformation

Hong He[1]

Yumiko Hirokawa[1]

Aviv Gazit[2]

Yoshihiro Yamashita[3]

Hiroyuki Mano[3]

Yuko Kawakami[4]

Kawakami[4]

Ching-Yi Hsieh[5]

Hsing-Jien Kung[5]

Guillaume Lessene[6]

Jonathan Baell[6]

Alexander Levitzki[2]

Hiroshi Maruta[1],*

[1]Ludwig Institute for Cancer Research; Royal Melbourne Hospital; Parkville/Melbourne, Australia

[2]Department of Biological Chemistry; The Alexander Silverman Institute of Life Sciences; Hebrew University of Jerusalem; Jerusalem, Israel,

[3]Division of Functional Genomics; Jichi Medical School; Tochigi, Japan

[4]La Jolla Institute for Allergy and Immunology; San Diego, California USA

[5]Cancer Center; University of California at Davis; Sacramento, California USA

[6]Walter and Eliza Hall Institute for Medical Research; Parkville/Melbourne, Australia

*Correspondence to: Hiroshi Maruta; Ludwig Institute for Cancer Research; P.O. Box 2008 Royal Melbourne Hospital; Parkville/Melbourne, Australia 3050; Tel.: 613.9341.3155; Fax: 613.9341.3104; Email: Hiroshi.maruta@ludwig.edu.au

ABSTRACT

AG 879 has been widely used as a Tyr kinase inhibitor specific for ErbB2 and FLK-1, a VEGF receptor. The IC_{50} for both ErbB2 and FLK-1 is around 1 μM. AG 879, in combination of PP1 (an inhibitor specific for Src kinase family), suppresses almost completely the growth of RAS-induced sarcomas in nude mice. In this paper we demonstrate that AG 879 even at 10 nM blocks the specific interaction between the Tyr-kinase ETK and PAK1 (a CDC42/ Rac-dependent Ser/Thr kinase) in cell culture. This interaction is essential for both the RAS-induced PAK1 activation and transformation of NIH 3T3 fibroblasts. However, AG 879 at 10 nM does not inhibit either the purified ETK or PAK1 directly in vitro, suggesting that this drug blocks the ETK-PAK1 pathway by targeting a highly sensitive kinase upstream of ETK. Although the Tyr-kinases Src and FAK are known to activate ETK directly, Src is insensitive to AG 879, and FAK is inhibited by 100 nM AG 879, but not by 10 nM AG879. The structure-function relationship analysis of AG 879 derivatives has revealed that both thio and tert-butyl groups of AG 879, but not (thio) amide group, are essential for its biological function (blocking the ETK-PAK1 pathway), suggesting that through the (thio) amide group, AG 879 can be covalently linked to agarose beads to form a bioactive affinity ligand useful for identifying the primary target of this drug.

INTRODUCTION

PAK1, a member of CDC42/Rac-dependent Ser/Thr kinase family (PAKs), is activated by oncogenic RAS mutants such as v-Ha-RAS, and is essential for RAS-transformation of fibroblasts such as Rat-1 and NIH 3T3 cells.[1,2] Several distinct pathways appear to be essential for v-Ha-RAS-induced activation of PAK1 in these cells.[2] One of these pathways involves PI-3 kinase which produces phosphatidyl-inositol 3,4,5 trisphosphate (PIP3) that activates both CDC42 and Rac GTPases through a GDP-dissociation stimulator (GDS) called VAV. A second pathway involves PIX, an SH3 protein which binds a Pro-rich motif (residues 186-203, PAK18) located between the N-terminal GTPase-binding domain and C-terminal kinase domain of PAK1.[3] PIX binds another protein called CAT which is a substrate of Src family kinases.[4] A third pathway involves an SH2/SH3 adaptor protein called NCK.[5] The SH3 domain of NCK binds another Pro-rich motif of PAK1 located near the N-terminus, while the SH2 domain of NCK binds the Tyr-phosphorylated EGF receptor/ErbB1.[5] Thus, when ErbB1 is activated by EGF, PAK1 is translocated to the plasma membrane through NCK. The involvement of both Src family kinases and ErbB1 in the PAK1 activation is also supported by our finding that both PP1 (inhibitor of Src family kinases) and AG1478 (ErbB1-specific inhibitor) block the RAS-induced PAK1 activation and transformation in vitro and in vivo.[2,6] A fourth pathway involves ErbB2, a member of ErbB family Tyr kinases.[2] We have previously shown that AG 825 (ErbB2-specific inhibitor) blocks RAS-induced activation of PAK1 and malignant transformation with the IC_{50} around 0.35 μM.[2] A fifth pathway has been recently discovered in which RAS activates PAK1 through Tiam1, a Rac-specific GDS , in a PI-3 kinase-independent manner.[7] In this pathway, RAS directly binds Tiam1 which in turn activates Rac.[7]

Another possible pathway involves β1-integrin, FAK and ETK. β1-integrin activates the Tyr kinase FAK, which in turn phosphorylates and activates ETK,[8] a member of TEC/BTK family Tyr kinases.[9,10] ETK carries an N-terminal pleckstrin homology (PH) domain followed by a TEC homology domain.[9,10] Activated ETK binds PAK1 through the PH domain, phosphorylates and activates PAK1.[11] However, it still remains to be

clarified (1) whether RAS requires this integrin/FAK/ ETK pathway for its oncogenicity, and (2) how RAS activates this pathway.

To suppress the growth of RAS-induced sarcomas in vivo (in nude mice), we previously used AG 879, a Tyr-kinase inhibitor specific for ErbB2 and VEGF receptor FLK-1.[2,12,13] In this paper we demonstrate that AG879 inhibits selectively the activation of ETK (IC_{50} around 5 nM), blocking RAS-induced ETK-mediated activation (Tyr phosphorylation) of PAK1 to suppress RAS transformation.

MATERIALS AND METHODS

Cell Culture and Reagents. v-Ha-RAS-transformed NIH 3T3 fibroblasts (RAS cells) were grown in a standard medium, i.e., Dulbecco's modified Eagle's medium in the presence or absence of 10% fetal calf serum as described previously.[2,6] The Tyr kinase inhibitor AG879 and its derivatives (AG 306 and AG 1584) were synthesized as described previously.[12] The novel derivative GL-2002 was synthesized analogously, and full synthetic details will be published in due course. Two other AG 879 derivatives (AG 99 and AG 213) were purchased from Calbiochem (Croydon, Australia). The following antibodies were obtained from Santa Cruz Biotechnology (Santa Cruz,CA): anti-PAK1 antibody, anti-phospho-Tyr antibody (PY99) and goat-anti-ETK antibody. The rabbit anti-FAK antibody was a generous gift of Dr. David Schlaepfer (The Scripps Research Institute, La Jolla, CA). The mouse anti-ETK antibody was purchased from Becton Dickinson Biosciences (North Ryde, NSW, Australia). The rabbit anti-ETK antibody was prepared as described previously.[14]

Assay for the Effect of AG 879 on Cell Growth. The effect of AG879 on anchorage-independent growth of RAS cells was determined by seeding 10^3 cells per plate into 0.35% top agar containing different concentrations of AG879 (from 1 nM to 1 μM) and incubating for 3 weeks as described previously.[2,6,15] At the end of 3 weeks, the colonies formed in the agar were stained and counted. The effect of AG 879 on anchorage-dependent growth of RAS cells and normal NIH/3T3 fibroblasts was examined by seeding 10^3 cells per plate in the medium containing 1–100 nM AG 879, incubating for 5 days and counting as described previously.[2,6,15]

PAK and ETK Kinase Assays. For the PAK kinase assay, RAS cells were serum-starved overnight, and then treated with different concentrations of AG879 for 1 hour as described in the text. The cells were lysed in the lysis buffer (40 mM HEPES, pH 7.4, 1% Nonidet P-40, 1 mM EDTA, 100 mM NaCl, 25 mM NaF, 100 μM NaVO₃, 1 mM phenylmethylsulfonyl fluoride (PMSF), and 100 units/ml aprotinin). The lysates containing 1 mg of proteins (measured by Bradford assay) were immuno-precipitated with the anti-PAK1 antibody, and the immuno-precipitates were subjected to the PAK kinase assay as described previously.[1,2,6,16] The direct effect of AG 879 on PAK1 was determined in vitro, using GST-PAK1 fusion protein as described previously.[17] For ETK kinase assay, serum-starved RAS cells were lysed in a buffer containing 20 mM Tris-HCl (pH 7.5), 100 mM NaCl, 10% glycerol, 1% Nonidet P-40, 10 mM NaF, 100 μM NaVO₃, 1 mM PMSF, and 100 units/ml aprotinin. The cell lysates were immuno-precipitated with the rabbit anti-ETK antibody, and the ETK kinase assay was performed as described previously[8,11] using the endogenous PAK1 associated with ETK as a substrate in the presence or absence of different concentrations of AG879 or its derivatives such as AG 1584. Immuno-blotting was performed to determine the protein levels for PAK1 and ETK (see below).

Immuno-Precipitation and Immuno-Blotting. Serum-starved RAS cells were treated with different concentrations of AG879 as indicated in the text. The cells were lysed in two different lysis buffers mentioned above. The cell lysates containing 1.5–2.0 mg of protein (measured by Bradford assay) were incubated with protein A-Sepharose beads (Amersham Pharmacia Biotech) and anti-PAK1, anti-ETK or anti-FAK antibodies separately.[2,8,11,18] The proteins in immuno-precipitates were separated on 4–12% NuPage gel (Invitrogen) electrophoresis and transferred to a nitrocellulose membrane

(Micron Separations, Inc.). The membranes were blocked with 10% (w/v) skim milk in phosphate-buffered saline containing 0.04% Tween20 (PBST), followed by an incubation for 1 hr at room temperature with different first antibodies as described in the text. After washing with PBST, the blots were incubated with horseradish peroxidase-conjugated anti-mouse or anti-rabbit (Bio-Rad) secondary antibodies. The bound antibodies were visualised using ECL reagents (Amersham Pharmacia Biotech). Some membranes were stripped and reblotted[19] with different antibodies as described in the text.

The ETK Baculo Viral Construct and its Affinity-Purification. The plasmid encoding the full-length ETK (residues 1-674)[14] was constructed in pBacPAK8 transfer vector (Clontech, Palo Alto, CA) and recombinant virus was made by Dr. Chi-Ying F. Huang (NHRI, Taiwan). Sf9 insect cells infected with the recombinant virus were harvested and disrupted with ice-cold lysis buffer containing 10 mM Tris pH, 7.5; 130 mM NaCl; 1% Triton X-100; 10 mM NaF; 10 mM Na phosphate; 10 mM Na pyro-phosphate and protease inhibitor cocktail (Pharmingen, San Diego, CA). From the clear supernatant of the cell lysate obtained by centrifuging at 40,000xg for 45 min, ETK was affinity-purified by the 6xHis purification kits (Cat. No. 21474K, Pharmingen, San Diego, CA) according to the supplier's instruction.

Autophosphorylation of Recombinant ETK Constructs In Vitro. GST fusion protein of human ETKC, a constitutively activated ETK mutant (residues 243–674) which lacks the N-terminal PH domain was affinity-purified from bacteria (E. coli). The GST-ETKC (0.6 μg) was incubated in the kinase buffer containing 10 μM ATP (with or without 5 μCi of [γ-³²P]-ATP) as described previously[8] in the presence or absence of AG879 (10 nM or 1–10 mM) at 37°C for 40 min. The auto-phosphorylation was then monitored by immuno-blotting the protein separated by the SDS-PAGE and transferred onto nitrocellulose with anti-phospho-Tyr antibody (or by radio-autography). Similarly 3 μg of full-length ETK purified from the insect cells was incubated in the buffer containing 30 mM PIPES, pH 7.0, 10 μM MnCl² , 30 μM ATP, 5 μCi of [γ -³²P] ATP, 1 mM Na₃VO₄ for 20 min at 30°C, in the presence or absence of AG879 (10 nM–1 mM), and the auto-phosphorylation was measured by radio-autography of the proteins separated on SDS-PAGE.

Upregulation of ETK by RAS. The ETK protein levels were compared between normal NIH/3T3 cells and two distinct v-Ha-RAS transformed cell lines, excluding the possible clonal difference in the ETK levels: stable v-Ha-RAS cell line (RAS cells) and doxycycline-inducible v-Ha-RAS transformants prepared as described previously.[20,21] The lysates of both normal and RAS cells (20 μg protein of each) were subjected to SDS-PAGE and immuno-blotted by the anti-ETK antibody. In the case of doxycycline-inducible RAS transformants, cells were incubated for 2–3 days in the presence or absence of 2 μg/ml doxycycline, and each lysate (20 μg protein) was subjected to the SDS-PAGE/ immuno-blot with the anti-ETK.

RESULTS

AG879 (10 nM) Blocks the Activation of PAK1 and Suppresses RAS-Induced Malignant Transformation. AG879 was reported as an inhibitor specific for both ErbB2 and VEGF receptor FLK-1 (IC50 is around 1 mM)[12,13] and appears to be metabolically more stable than AG825 in vivo as it strongly suppresses the growth of RAS-sarcomas in nude mice.[2] However, the IC_{50} of AG879 for inhibiting PAK1 activation and RAS transformation in vitro still remained to be determined.

10 nM AG879 strongly blocks PAK1 kinase activity in RAS cells without affecting the PAK1 protein level (Fig. 1A). However, AG879 does not inhibit the kinase activity of the purified GST-PAK1 fusion protein directly even at 1 μM (Fig. 1B). These observations suggest that ErbB2 is not involved in the inactivation by AG879 of PAK1 in cells. Interestingly, AG879 also suppresses the anchorage-independent growth of RAS cells in soft agar (Fig. 1C). The IC_{50} of AG879 for the large colony formation is 1–10 nM. However, the inhibition of anchorage-independent growth by AG879 is not due to non-specific inhibition on cell growth, as at even 100
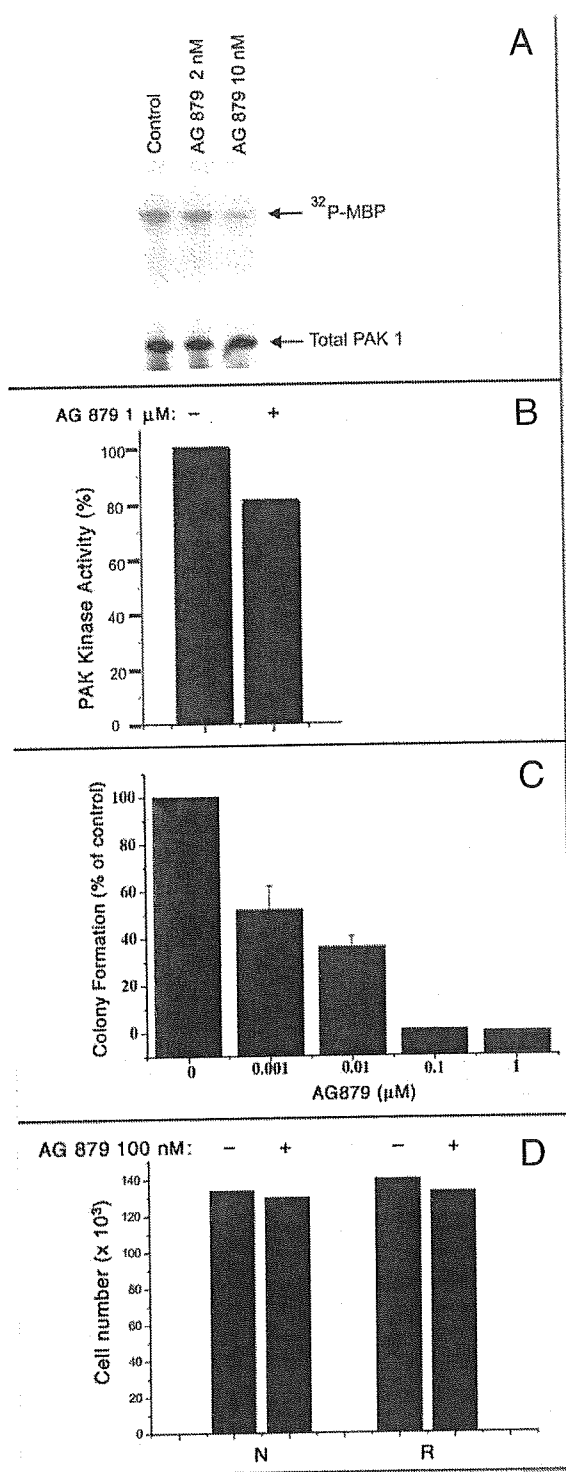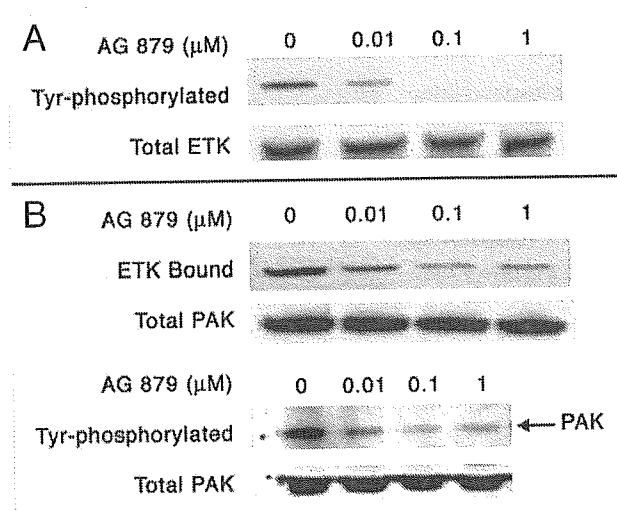
Figure 2. AG879 blocks the Tyr-phosphorylation of ETK and its association with PAK1. (A) Serum-starved RAS cells were first incubated with AG879 (0.01-1 μM) for 1hr. The cells lysates (CL) were then immuno-precipitated (IP) with the anti-ETK antibody as described under "Materials & Methods", followed by immuno-blot (IB) with anti-phospho-Tyr (PY) antibody. (B) Alternatively, the CL were IP with the anti-PAK1 (top panel) or anti-PY (bottom panel) antibodies, followed by IB with anti-ETK (top panel) or anti-PAK1 (bottom panel) antibodies. The total PAK1 protein level of the bottom panel was determined by IBing each CL directly. Similar results were obtained from two or three independent experiments.

nM AG879 does not affect the anchorage-dependent growth of either normal or RAS-transformed NIH 3T3 cells (Fig. 1D). These results suggest that the suppression by AG 879 of both RAS-induced malignant transformation and PAK1 activation is not due to blocking ErbB2, but another kinase(s) associated with PAK1.

AG879 Inhibits the Tyr-Phosphorylation of ETK and Its Association with PAK1. The Tyr-phosphorylation of PAK1 is required for its Ser/Thr kinase activity as the treatment of PAK1with a Tyr-phosphatase reduces its kinase activity.[22] Activated ETK associates with PAK1 through its PH domain and activates PAK1 by the Tyr phosphorylation.[11] To test whether the Tyr kinase activity of ETK is affected by AG879, serum-starved RAS cells were treated with AG879 (0.01-1 μM) in culture for 1hr. Cell lysates were then immuno-precipitated with the anti-ETK antibody, followed by immuno-blotting with the anti-phospho-Tyr or anti-ETK antibody. AG879 inhibits the Tyr-phosphorylation of ETK at 10 nM, but does not affect the ETK protein level (Fig. 2A). Furthermore, using the anti-PAK1 antibody, we found that AG879 significantly suppresses the ETK-PAK1 association (Fig.2B, top panel) and reduced the Tyr-phosphorylation of PAK1 in cells at 10 nM (Fig.2B, bottom panel). These results suggest that AG879 inhibits somehow the kinase activity of ETK, thus blocking its auto-phosphorylation, and association with PAK1, and the Tyr-phosphorylation of PAK1 by ETK.

AG879 Inactivates ETK In Vitro. To determine whether AG879 directly inhibits the kinase activity of ETK or not, RAS cells were lysed and

Figure 1. (A) AG879 inhibits the activation of PAK1 in cells. Serum-starved RAS cells were incubated with AG879 (0.01-10 μM) for 1hr. The cell lysates were subjected to PAK kinase assay as described under "Materials & Methods". 10 nM AG 879 clearly inhibited the PAK1 activity (phosphorylation of MBP) in cells (top panel). Similar levels of PAK1 protein were detected in all lanes as judged by immuno-blot (bottom panel). (B) PAK1 is not a direct target of AG 879. 1 μM AG 879 fails to inhibit significantly the kinase activity of GST-PAK1 in vitro. (C) AG879 inhibits anchorage-independent growth of RAS cells. RAS cells were planted in soft agar with or without AG879 (0.001-100 μM) as described under "Materials & Methods". The colony formation was measured in comparison with that of the control (non-treated) cells. Only large colonies consisting more than 100 cells per colony were counted. The presented values are the average of those obtained from two independent experiments. (D) AG 879 has no effect on the anchorage-dependent cell growth. The growth of either normal or RAS-transformed cells in liquid culture was monitored in the presence or absence of 100 nM AG 879 as described under "Materials & Methods".

A

Tyr-phosphorylated   0   10   100   AG879 (nM) ← PAK

Total ETK ←

B

AG879 (nM)   0   1   5   10

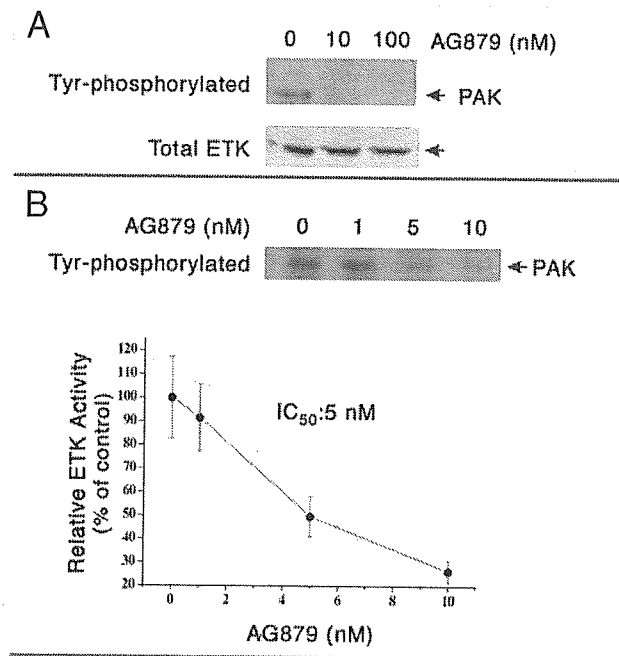Tyr-phosphorylated   ← PAK

IC$_{50}$:5 nM

Figure 3. AG879 inhibits the kinase activity of ETK in vitro. The lysates of RAS cells were immuno-precipitated by anti-ETK antibody. The immuno-precipitates (IB) were subjected to an in vitro kinase assay in the presence or absence of AG879 (A, 10 or 100 nM; B, 1 to 10 nM) as described under "Materials & Methods". The ETK activity (Tyr-phosphorylation of PAK1) was monitored by immuno-blot (IB) with anti-PY antibody. Similar protein levels of ETK were detected in all lanes by IB with the anti-ETK antibody. Similar results were obtained from two independent experiments.

immuno-precipitated with the anti-ETK antibody. The immuno-precipitates were subjected to an in vitro kinase assay in the presence or absence of AG879 (0.001–10 μM) as described in the "Materials and Methods". AG879 (10 nM) strongly inhibits the Tyr-phosphorylation of PAK1 by

Figure 5. AG879 suppresses the Tyr-phosphorylation of FAK and its association with ETK and PAK1. Serum-starved RAS cells were incubated with AG879 (0.01–1 μM) for 1hr. The cell lysates were immuno-precipitated (IP) with anti-FAK antibody as described under "Materials & Methods", followed by immuno-blot (IB) with anti-phospho-Tyr (PY), anti-ETK or anti-PAK antibodies. Similar protein levels were detected in all lanes by IB with the anti-FAK antibody. Similar results were obtained from two independent experiments.

ETK (Fig.3A), and the IC$_{50}$ for ETK is around 5 nM (Fig. 3B). Furthermore, AG 879 has no direct effect on any other members of TEC family kinases such as TEC, BTK or ITK, even at 10 μM in vitro (data not shown). These results suggest that ETK is so far most sensitive to the action of AG879. However, since the anti-ETK antibody could precipitates not only ETK itself, but also any proteins forming a tight complex with ETK such as PAK1 and FAK, we cannot exclude the possibility that the primary target of AG 879 might be a third Tyr-kinase which is associated with ETK, and responsible for the ETK activation.

AG879 (5 nM) Does Not Inhibit Recombinant ETK from Bacteria or Insect Cells. To clarify whether ETK itself is the primary target of ETK, two different recombinant ETK samples of human origin were purified from bacteria or insect cells: a constitutively activated mutant of ETK called ETKC (residues 243–674) which lacks the N-terminal PH domain purified from bacteria as a GST fusion protein, and full-length ETK purified from insect cells. Either the ETKC or the full-length ETK were not inhibited by AG 879 at 10 nM, although they were significantly inhibited at 1–10 μM (see Fig. 4). Furthermore, in vitro binding of PAK1 in RAS cell lysates to either the PH domain of ETK or a kinase-dead mutant of ETK (called
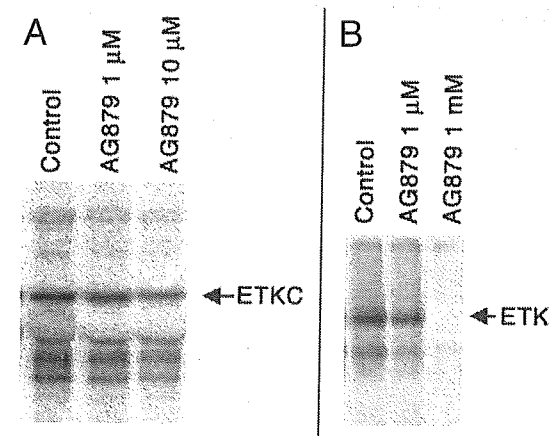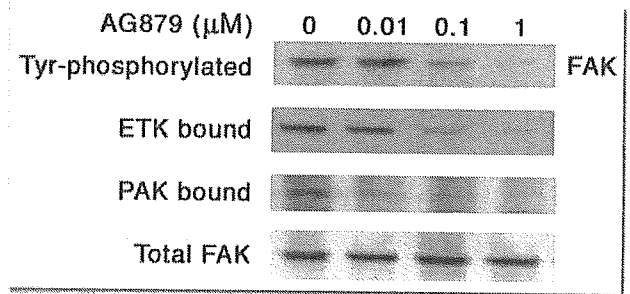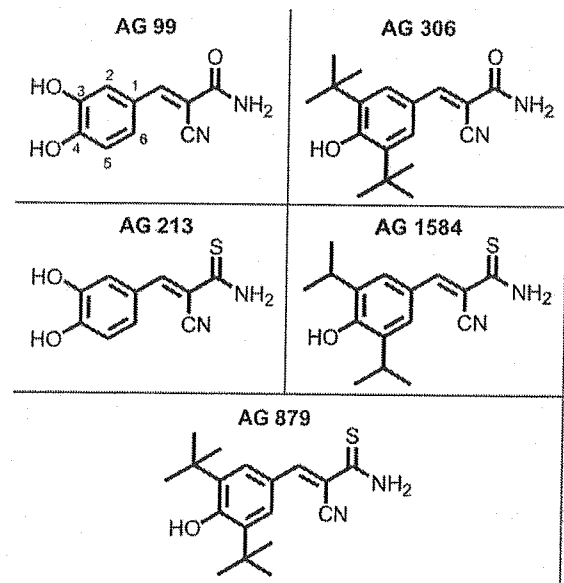

Figure 4. Recombinant ETK proteins alone are far less sensitive to AG 879 in vitro. (A) Effect of AG879 on the ETKC from bacteria. The GST-ETKC was auto-phosphorylated in the presence of AG 879 (0, 1 and 10 μM) in vitro as described under "Materials and Methods". (B) Effect of AG879 on full-length ETK from insect cells. The full-length ETK was auto-phosphorylated in the presence of AG 879 (0, 1 μM and 1mM) in vitro as described under "Materials and Methods".

Figure 6. Chemical structure of AG 879 derivatives.

Figure 8. RAS-induced up-regulation of ETK. Upper panel: Up-regulation of ETK by the Doxycyline-induced v-Ha-RAS expression in normal NIH/3T3 cells. Dox-minus, the control (no doxycycline-added); Dox-plus, 2 μg/ml doxycycline added. Lower panel: Enhanced expression of ETK in v-Ha-RAS-transformants. N, normal NIH/3T3 cells; R, v-Ha-RAS-transformants. The arrow indicates the ETK band. Both stable and inducible RAS up-regulate the ETK protein level.

Figure 7. Anti-ETK activity of AG 879 derivatives. (A) The lysates of RAS cells were immuno-precipitated by anti-ETK antibody. The immuno-precipitates (IP) were subjected to an in vitro kinase assay in the absence of any drug (CONT) or presence of either AG879 (10 nM) or four other derivatives (10 μM) as described in Figure 3. Only AG 879 inhibits the ETK activity (Tyr-phosphorylation of PAK1) monitored by immuno-blot (IB) with anti-PY antibody. Similar protein levels of ETK were detected in all lanes by IB with the anti-ETK antibody. Similar results were obtained from two independent experiments. (B) After RAS cells were treated with either 10 nM GL-2002 or AG 879 for 1.5 hrs, each cell lysate was subjected to the in vitro PAK1 kinase assay described in Fig. 1B. GL-2002 strongly inhibited PAK1 activation as did AG 879. Similar results were obtained from three independent experiments.

ETK/KQ) as a GST-fusion protein was not inhibited by 10 nM AG879 (Hirokawa Y, He H, Maruta H, unpublished observation, 2002). These observations altogether suggest that the primary target of AG879 is not ETK itself, but rather its associated upstream activator to be identified.

AG879 Inhibits the Tyr-Phosphorylation of FAK and Its Association with ETK and PAK1. ETK is a cytoplasmic (non-receptor) Tyr kinase which is activated at the plasma membranes.[9,10] The N-terminus of FAK shares significant sequence homology with FERM domains, which are involved in linking cytoplasmic proteins to the membranes.[23,24] It was shown recently that the activation of ETK by extracellular matrix (ECM) is regulated by FAK through the interaction between the PH domain of ETK and the FERM domain of FAK, and that activated FAK binds ETK and elevates the Tyr-phosphorylation of ETK.[8]

To test whether the FAK-ETK interaction is affected by AG879, serum-starved RAS cells were treated with AG879 (0.01–1μM). Cell lysates were then immuno-precipitated with anti-FAK antibody, followed by blotting with anti-phospho-Tyr, anti-ETK or anti-PAK1 antibodies separately. As shown in Figure 5, AG879 suppresses both the Tyr-phosphorylation of FAK and its association with ETK at 100 nM, but not at 10 nM, whereas AG879
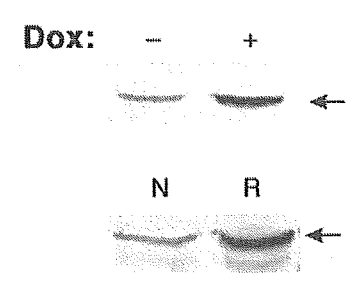
inhibits the FAK-PAK1 interaction at 10 nM. These results suggest that PAK1 associates with FAK probably through ETK, and PAK1 can no longer interact with FAK when the PAK1-ETK complex is disrupted by AG879.

The Structure-Function Analysis of AG879 Derivatives in Inhibiting ETK. To determine which side chains of AG879 are essential for the ETK inhibition, and further screen for a more potent "ETK inhibitor", we have examined the anti-ETK activity of several AG879 derivatives shown in Figure 6. However, none of these derivatives other than AG879 itself inhibits ETK activity in vitro even at 10 μM (see Fig. 7A). These results indicate that at least both tert butyl groups at positions 3 and 5, and the thio group are absolutely essential for AG879 to inhibit ETK. Interestingly, the ErbB2-specific inhibitor AG825 is distantly related to AG879, but like AG306, lacks both the thio and tert butyl groups, and in fact shows no anti-ETK activity at even 1 μM in vitro (data not shown). However, when the free (thio) amino group of AG879 was alkylated with an amino-hexane chain, the resulting derivative called GL-2002 was still able to show a strong anti-ETK activity that blocks the PAK1 activation in RAS cells even at 10 nM (Fig. 7B), suggesting that, unlike other side chains, this free amino group of AG879 is not essential for its anti-ETK activity. Thus, we are currently generating a series of bioactive immobilized AG 879 (or its water-soluble N-hexylamine derivative, called GL-2003) by coupling them to agarose beads through the amino group so that we can use the AG879/GL-2003 bead as a ligand for fishing a high-affinity AG879-binding protein(s).

Upregulation of ETK Protein Level by RAS. How does RAS activate this integrin/FAK/ETK pathway? Although the whole picture of this mechanism still remains to be unveiled, we found that v-Ha-RAS upregulates the protein level of ETK several folds, using both doxycycline-inducible v-Ha-RAS transformants and stable v-Ha-RAS transformants derived from normal NIH/3T3 cells (see Fig. 8), clearly indicating that oncogenic RAS signalling involves ETK.

DISCUSSION

In this study, we have demonstrated that AG879 selectively inactivates the cytoplasmic Tyr kinase ETK with IC_{50} of about 5 nM. The inactivation of ETK by AG879 blocks the ETK-PAK1 interaction, thereby blocking the Tyr-phosphorylation of PAK1 and its kinase activity. Interestingly at this concentration AG879 does not inhibit directly any other kinases including FAK, PAK, ErbB2, ErbB1, TRK, TEC, BTK and ITK. However, since the IC_{50} of this drug for recombinant ETK proteins alone is 1–10 μM, instead of 5 nM, it is most likely that the primary target of AG879 is not ETK, FAK or ErbB2 themselves, but an as yet unidentified activator of ETK. Thus, we are currently identifying this highly AG879-sensitive

target among the kinases which are associated with ETK, Tyr-phosphorylate the kinase-dead (non-auto-phosphorylatable) mutant of ETK (ETK-KQ), and bind tightly to the AG879/GL-2003 beads. Our preliminary data suggest that the primary target is a Tyr-phosphorylated protein of 62 kDa (Hirokawa Y and Maruta H, unpublished observation).

ETK is required for the anchorage-independent and tumorigenic growth of human breast cancer cells.[11] Although ETK alone is not transforming, it enhances malignant transformation of NIH 3T3 cells caused by a partially activated c-Src mutant.[25] ETK can also be activated by Src family kinases and is responsible for Src activation of signal transducer and activator of transcription factor 3 (STAT3) and v-Src-induced transformation.[25] In this study we have established that ETK is essential for RAS transformation: the concentration of AG879 that inhibits both RAS-induced PAK1 activation and anchorage-independent growth is similar to the IC_{50} for ETK both in vitro and in vivo.

We have established here that RAS signalling involves ETK by demonstrating that RAS significantly up-regulates the ETK protein level. To understand further the detailed mechanism, we are currently investigating whether this regulation is at either transcriptional or translational levels or its stability (turn-over rate). In this context, it is worth noting that ETK is highly expressed in metastatic prostate and breast carcinoma cell lines such as PC3M which carry oncogenic Ki-RAS mutants.[8] Since RAS cells in general are both metastatic and angiogenic, it is conceivable that at least a part of the reason for the high expression of ETK in these cell lines might be due to the constitutive RAS activation. Thus, it would be of great interest to determine whether AG879 inhibits the metastasis of these RAS cancer cell lines in vivo.

It was suggested earlier that AG879 (also called SU0879) suppresses angiogenesis by blocking VEGF receptor FLK-1.[13] However, since the VEGF receptor also directly activates ETK[10] which is then inhibited by AG879 at 5 nM (200 times more sensitive to this drug than FLK-1), it is more likely that AG879 suppresses angiogenesis primarily by blocking ETK, rather than FLK-1. Since oncogenic RAS mutants up-regulate expression of VEGF through Raf-MEK-MAP kinase cascade,[26] and VEGF in turn activates ETK through FLK-1in endothelial cells, RAS transformation can induce angiogenesis through this paracrine pathway. Thus, it is conceivable that the suppression of RAS sarcomas growth by AG879 in mice[2] might be at least in part due to its anti-angiogenic action, (in addition to blocking the anchorage-independent growth of RAS cells per se). Interestingly it was recently shown that PAK1 is essential for angiogenesis. A cell-permeable peptide which blocks selectively the NCK-PAK1 interaction inhibits bFGF-induced angiogenesis.[27]

References

1. Tang Y, Chen Z, Ambrose D, Liu J, Gibbs JB, Chernoff J, Field J. Kinase-deficient Pak1 mutants inhibit Ras transformation of Rat-1 fibroblasts. Mol Cell Biol 1997; 17:4454-64.
2. He H, Hirokawa Y, Manser E, Lim L, Levitzki A, Maruta H. Signal therapy for RAS-induced cancers in combination of AG 879 and PP1, specific inhibitors for ErbB2 and Src family kinases, that block PAK activation. Cancer J 2001 7:191-202.
3. Manser E., Loo TH, Koh CG, et al. PAK kinases are directly coupled to the PIX family of nucleotide exchange factors. Mol Cell 1998; 1:183-92.
4. Bagrodia S, Bailey, D, Lenard, Z, et al. A tyrosine-phosphorylated protein that binds to an important regulatory region on the cool family of p21-activated kinase-binding proteins. J Biol Chem. 1999; 274:22393-400.
5. Galisteo M, Chenoff J, Su YC, et al. The adaptor protein Nck links receptor tyrosine kinases with the serine-threonine kinase Pak1. J Biol Chem 1996; 271:20997-1000.
6. He H, Hirokawa Y, Levitzki A, Maruta H. An anti-Ras cancer potential of PP1, an inhibitor specific for Src family kinases: in vitro and in vivo studies. Cancer J 2000; 6:243-8.
7. Lambert J, Lambert Q, Reuther G, Malliri A, Siderovski D, Sondek J, et al. Tiam1 mediates RAS activation of Rac by a PI-3 kinase-independent mechanism. Nat Cell Biol 2002; 4:621-5.
8. Chen R, Kim O, Li M, Xiong X, Guan JL, Kung HJ, et al. Regulation of the PH-domain-containing tyrosine kinase Etk by focal adhesion kinase through the FERM domain. Nat Cell Biol 2001; 3:439-44.
9. Qiu Y, Kung HJ. Signaling network of the Btk family kinases. Oncogene 2000; 19:5651-61.
10. Smith CI, Islam TC, Mattsson PT, Mohamed AJ, Nore BF, Vihinen M. The Tec family of cytoplasmic tyrosine kinases: mammalian Btk, Bmx, Itk, Tec, Txk and homologs in other species. Bioessays 2001; 23:436-46.
11. Bagheri-Yarmand R, Mandal M, Taludker AH, Wang RA, Vadlamudi RK, Kung HJ, Kumar R. Etk/Bmx tyrosine kinase activates Pak1 and regulates tumorigenicity of breast cancer cells. J Biol Chem 2001; 276:29403-9.
12. Levitzki A, Gazit A. Tyrosine kinase inhibition: an approach to drug development. Science 1995; 267:1782-8.
13. Strawn L, McMahon G, App H, Schreck R, et al. Flk-1 as a target for tumor growth inhibition. Cancer Res 1996; 56:3540-5.
14. Qiu Y, Robinson D, Pretlow T, Kung HJ. Etk/Bmx, a tyrosine kinase with a pleckstrin-homology domain, is an effector of phosphatidylinositol 3'-kinase and is involved in interleukin 6-induced neuroendocrine differentiation of prostate cancer cells. Proc Natl Acad Sci USA 1998; 95:3644-9.
15. Maruta H, Holden J, Sizeland A, D'Abaco G. The residues of Ras and Rap proteins that determine their GAP specificities. J Biol Chem 1991; 266:11661-8.
16. Obermeier A, Ahmed S, Manser E, Yen SC, Hall C, Lim L. PAK promotes morphological changes by acting upstream of Rac. EMBO J 1998; 17:4328-39.
17. Nheu T, He H, Hirokawa Y, Tamaki K, et al. The K252a derivatives, inhibitors for the PAK/MLK kinase family, selectively block the growth of RAS transformants. Cancer J 2002; 8:328-35.
18. Bellis SL, Miller JT, Turner CE. Characterization of tyrosine phosphorylation of paxillin in vitro by focal adhesion kinase. J Biol Chem 1995; 270:17437-41.
19. He H, Levitzki A, Zhu HJ, Walker F, Burgess A, Maruta H. Platelet-derived growth factor requires epidermal growth factor receptor to activate p21-activated kinase family kinases. J Biol Chem 2001; 276: 26741-4.
20. Zhu HJ, Iaria J, Sizeland A. Smad7 differentially regulates TGF-β-mediated signalling pathways. J Biol Chem 1999; 274:32258-64.
21. Zhu HJ, Nheu T, Cheng HC, Iaria J, Simpson R, Maruta H, Burgess AW. Oncogenic RAS transformation downregulates the expression of the PTEN tumor suppressor. Cancer Res 2003; In press.
22. McManus MJ, Boerner JL, Danielsen AJ, Wang Z, Matsumura F, Maihle NJ. An oncogenic epidermal growth factor receptor signals via a p21-activated kinase-caldesmon-myosin phosphotyrosine complex. J Biol Chem 2000; 275:35328-34.
23. Chishti AH, Kim AC, Marfatia SM, et al. The FERM domain: a unique module involved in the linkage of cytoplasmic proteins to the membrane. Trends Biochem Sci 1998; 23:281-2.
24. Girault JA, Labesse G, Mornon JP, Callebaut I. The N-termini of FAK and JAKs contain divergent band 4.1 domains. Trends Biochem Sci 1999; 24:54-7.
25. Tsai YT, Su YH, Fang SS, Huang TN, Qiu Y, Jou YS, Shih HM, Kung HJ, Chen RH. Etk, a Btk family tyrosine kinase, mediates cellular transformation by linking Src to STAT3 activation. Mol Cell Biol 2000; 20:2043-54.
26. Grugel S, Finkenzeller G, Weindel K, et al. Both v-Ha-Ras and v-Raf stimulate expression of the vascular endothelial growth factor in NIH 3T3 cells. J Biol Chem. 1995;270:25915-9.
27. Kiosses W, Hood J, Yang S, et al. A dominant-negative PAK peptide inhibits angiogenesis. Circ Res 2002; 90:697-702.

Reprogramming of human postmitotic neutrophils into macrophages by growth factors

Hiroto Araki, Naoyuki Katayama, Yoshihiro Yamashita, Hiroyuki Mano, Atsushi Fujieda, Eiji Usui, Hidetsugu Mitani, Kohshi Ohishi, Kazuhiro Nishii, Masahiro Masuya, Nobuyuki Minami, Tsutomu Nobori, and Hiroshi Shiku

It is generally recognized that postmitotic neutrophils give rise to polymorphonuclear neutrophils alone. We obtained evidence for a lineage switch of human postmitotic neutrophils into macrophages in culture. When the CD15$^+$CD14$^-$ cell population, which predominantly consists of band neutrophils, was cultured with granulocyte macrophage–colony-stimulating factor, tumor necrosis factor-α, interferon-γ, and interleukin-4, and subsequently with macrophage colony-stimulating factor alone, the resultant cells had morphologic, cytochemical, and phenotypic features of macrophages. In contrast to the starting population, they were negative for myeloperoxidase, specific esterase, and lactoferrin, and they up-regulated nonspecific esterase activity and the expression of macrophage colony-stimulating factor receptor, mannose receptor, and HLA-DR. CD15$^+$CD14$^-$ cells proceeded to macrophages through the CD15$^-$CD14$^-$ cell population. Microarray analysis of gene expression also disclosed the lineage conversion from neutrophils to macrophages. Macrophages derived from CD15$^+$CD14$^-$ neutrophils had phagocytic function. Data obtained using 3 different techniques, including Ki-67 staining, bromodeoxyuridine incorporation, and cytoplasmic dye labeling, together with the yield of cells, indicated that the generation of macrophages from CD15$^+$CD14$^-$ neutrophils did not result from a contamination of progenitors for macrophages. Our data show that in response to cytokines, postmitotic neutrophils can become macrophages. This may represent another differentiation pathway toward macrophages in human postnatal hematopoiesis. (Blood. 2004;103:2973-2980)

© 2004 by The American Society of Hematology

Introduction

One apparent characteristic of the hematopoietic system is that all types of mature cells with distinct functions are continuously replaced by cells derived from hematopoietic stem cells that reside mainly in the bone marrow and have the ability for self-renewal and multilineage differentiation.[1,2] In the process of differentiation, hematopoietic stem cells sequentially lose multilineage potential and generate lineage-committed progenitors with limited developmental capacity. Lineage-committed progenitors give rise to precursors that eventually differentiate into mature blood cells. After commitment to specific lineages, hematopoietic progenitor cells are incapable of producing mature cells of other lineages. For example, neutrophilic monopotent progenitors proliferate and differentiate into neutrophils, and progenitors restricted to a macrophage lineage cannot give rise to mature cells other than macrophages.

Several studies have focused on a lineage switch in the hematopoietic differentiation pathway. Boyd and Schrader[3] reported that murine pre–B-cell lines differentiate into macrophage-like cells in response to the demethylating drug, 5-azacytidine. B-lineage cells have been also shown to transit into neutrophils or natural killer (NK)/T-lineage cells.[4-8] Furthermore, the macrophage cell line differentiates into B-lineage cells.[9] Common lymphoid progenitors that exogenously express cytokine receptors or transcriptional factors develop myeloid lineage cells.[10-12] In addition to these lineage switches, lineage conversions within myeloid lineages have also been observed in experiments using cell lines and transformed cells. Enforced expression of transcriptional factors such as GATA-1 and PU.1 leads to the lineage switch of myeloid cells to cells with another myeloid phenotype.[12-17] These lineage switches include myeloid to megakaryocytic, myeloid to eosinophilic, myeloid to erythroid, and erythroid to myeloid conversions. The ectopic expression of PU.1 and C/EBP also results in the commitment of hematopoietic progenitors to an eosinophilic lineage.[18-20] With respect to normal primary cells, it has been reported that murine B-cell precursor cells acquire the potential to differentiate into macrophage-like cells when they are transferred to myeloid culture conditions.[21] Normal murine early T progenitor cells also generate macrophages in cultures supplemented with conditioned medium from a thymic stromal cell line or in the presence of cytokines.[22] Thus, normal murine lymphoid progenitors may retain the potential to differentiate into macrophages. Reynaud et al[23] reported that human cord blood–derived pro-B cells with DJ$_H$ rearrangements of the immunoglobulin (Ig) locus generate macrophages, NK cells, and T cells. However, it is unknown whether the lineage switch occurs in normal human mature hematopoietic cells.

We conducted research to determine whether normal postmitotic neutrophils are able to differentiate into other types of mature

cells. We found that human postmitotic neutrophils switched their differentiation program and acquired the features of macrophages in cultures supplemented with cytokines. These data support the possibility that postmitotic neutrophils commonly thought to be restricted to the neutrophilic differentiation pathway can become macrophages, and we argue that the lineage switch of human mature blood cells may, at least in part, be relevant to normal hematopoietic differentiation.

Materials and methods

Cytokines

Recombinant human macrophage colony-stimulating factor (M-CSF) and interferon-γ (IFN-γ) were purchased from R&D Systems (Minneapolis, MN). Recombinant human granulocyte macrophage–colony-stimulating factor (GM-CSF) was provided by Kirin Brewery (Tokyo, Japan). Recombinant human tumor necrosis factor-α (TNF-α) was a gift from Dainippon Pharmaceutical (Suita, Japan). Recombinant human interleukin-4 (IL-4) was provided by Ono Pharmaceutical (Osaka, Japan). Cytokines were used at the following concentrations: M-CSF, 100 ng/mL; IFN-γ, 25 IU/mL; GM-CSF, 10 ng/mL; TNF-α, 20 ng/mL; and IL-4, 10 ng/mL.

Cell preparation

Peripheral blood was obtained from healthy Japanese donors given subcutaneous injections of granulocyte colony-stimulating factor (G-CSF) to harvest peripheral blood stem cells. Each donor gave written, informed consent. Peripheral blood mononuclear cells (PBMCs) were separated by centrifugation on Ficoll-Hypaque, washed with Ca^{2+}-, Mg^{2+}-free phosphate-buffered saline (PBS), and suspended in PBS with 0.1% bovine serum albumin (BSA) (Sigma Chemical, St Louis, MO). $CD15^+CD14^-$ cells were separated from PBMCs using CD14 and CD15 immunomagnetic beads (MACS; Miltenyi Biotec, Auburn, CA), according to the manufacturer's instructions. $CD14^+$ and $CD8^+$ cells were also separated from PBMCs using CD14 and CD8 immunomagnetic beads (MACS; Miltenyi Biotec), respectively. Healthy donors gave written, informed consent. The purity of $CD15^+CD14^-$, $CD14^+$, or $CD8^+$ cells exceeded 99%.

Culture

Culture medium was RPMI 1640 (Nissui Pharmaceutical, Tokyo, Japan) supplemented with 2 mM L-glutamine, 50 U/mL penicillin, 50 μg/mL streptomycin, and 10% fetal bovine serum (FBS) (HyClone Laboratories, Logan, UT). $CD15^+CD14^-$ cells (1 × 10⁶/mL) were cultured with designated combinations of cytokines in a 24-well tissue culture plate (Nunc, Roskilde, Denmark) for 18 days. Half of the culture medium was replaced with fresh medium containing cytokines every 3 to 4 days. In some experiments, cells were plated with designated combinations of cytokines; on day 11 of culture, the cells were washed 3 times with PBS and replated in cultures containing M-CSF. $CD14^+$ and $CD15^+CD14^-$ cells (1 × 10⁶/mL) were cultured in the presence of M-CSF for 7 days. Viable cells were counted using trypan blue dye exclusion methods.

Morphologic cell analysis

Cytospin preparations of freshly isolated and cultured cells were stained with May-Grünwald-Giemsa solution, myeloperoxidase (MPO) staining kit, and double-specific (naphthol AS-D chloroacetate esterase)/nonspecific (α-naphthyl butyrate esterase) esterase staining kit.

Cell cycle analysis

Cell cycle analysis was made using the CycleTEST PLUS DNA Reagent Kit (Becton Dickinson, San Jose, CA) according to the manufacturer's instructions. Nuclear DNA content of freshly isolated $CD15^+CD14^-$ cells was analyzed on a FACSCalibur flow cytometer (Becton Dickinson) with ModFit software (Verity Software House, Topsham, ME). HPB-NULL cells

(American Type Culture Collection, Manassas, VA) were used as a control. HPB-NULL cells were passaged every 24 hours for 3 days before use to minimize differences among experimental conditions.

Flow cytometric analysis

The following murine or rat monoclonal antibodies (mAbs) were used: anti–CD14-phycoerythrin (anti–CD14-PE), anti–CD15-fluorescein isothiocyanate (anti–CD15-FITC), and anti–HLA-DR-PE (Becton Dickinson); anti–MPO-FITC (DAKO, Glostrup, Denmark); anti–lactoferrin-PE (Immunotech, Marseille, France); anti–c-fms/M-CSF receptor (anti–c-fms/M-CSFR) (Oncogene Research, Boston, MA); anti–mannose receptor-PE, anti–Ki-67-FITC, which reacts with a proliferation-associated nuclear antigen, antibromodeoxyuridine (anti-BrdU)–FITC, and anti–rat IgG2b-FITC (Becton Dickinson PharMingen, San Diego, CA). Rat immunoglobulin and FITC- or PE-labeled mouse immunoglobulin served as isotype control: rat IgG2b and mouse IgM-FITC (Becton Dickinson PharMingen); mouse IgG1-FITC, IgG1-PE, and IgG2a-PE (Becton Dickinson); and mouse IgG2b-PE (Coulter, Miami, FL).

For membrane staining, cells were incubated with mAbs for 30 minutes on ice and washed 3 times with PBS. Intracellular molecules were stained, using Cytofix/Cytoperm Kit (PharMingen, San Diego, CA). Cells were fixed for 20 minutes at 4°C with formaldehyde-based fixation medium, washed, resuspended in permeabilization buffer containing sodium azide and saponin, and stained with mAbs for 30 minutes at 4°C. Cells were washed with the permeabilization buffer and PBS. HPB-NULL cells were used as a positive control for Ki-67 staining. Flow cytometric analysis was performed, using a FACSCalibur flow cytometer. CellQuest software (Becton Dickinson) was used for data acquisition and analysis.

BrdU and carboxyfluorescein diacetate succinimidyl ester (CFSE) labeling

For BrdU pulse labeling, freshly isolated and cultured cells (1 × 10⁶/mL) were incubated with 5 μg/mL BrdU (Sigma Chemical) for 40 minutes. The cells were washed with 0.1% BSA PBS, fixed with ice-cold 70% ethanol for 30 minutes at −20°C, and treated with 4 N HCl/0.5% Tween-20 at room temperature for 20 minutes for DNA denaturation. Acid was neutralized with 0.1 M $Na_2B_4O_7$. After washing with 0.1% BSA PBS, the cells were stained with FITC-conjugated anti-BrdU mAb. BrdU incorporation was analyzed using a FACSCalibur cytometer.[24] HPB-NULL cells served as a positive control for BrdU labeling.

Freshly isolated $CD15^+CD14^-$ cells (1 × 10⁶/mL) were labeled for 10 minutes at 37°C with 0.5 μM CFSE (Lambda, Graz, Austria) PBS, a cytoplasmic dye that is equally diluted between daughter cells, and were washed 3 times with 10% FBS RPMI 1640. CFSE-labeled $CD15^+CD14^-$ cells were cultured as described above. $CD8^+$ cells (1 × 10⁶/mL) were labeled with CFSE, washed with 10% FBS RPMI 1640, and cultured with T-cell expander beads (CD3/CD28 T-cell expander; DynalBiotech, Oslo, Norway) at a 1:3 bead-to-cell ratio for 5 days. CFSE-labeled freshly isolated and cultured cells were analyzed for fluorescence intensity using a FACSCalibur cytometer.[25]

Microarray

Microarray assay was carried out as described.[26,27] Total RNA extracted from freshly isolated and cultured cells by the acid guanidinium method was used to synthesize double-stranded cDNA. Biotin-labeled cRNA was prepared from each cDNA by ENZO BioArray High-Yield RNA Transcript Labeling kit (Affymetrix, Santa Clara, CA), and hybridized with a GeneChip HGU133A microarray (Affymetrix) harboring more than 22 000 human probe sets. Hybridization, washing, and detection of signals on the arrays were performed using the GeneChip system (Affymetrix) according to the manufacturer's protocols. Fluorescence intensity for each gene was normalized on the basis of the median expression value of the positive control genes (Affymetrix; HGU133Anorm.MSK) in each hybridization. Every microarray analysis was repeated twice. Hierarchical clustering and Welch analysis of variance (ANOVA) of the data set were conducted by using GeneSpring 6.0 software (Silicon Genetics, Redwood, CA).

Phagocytosis

Cultured cells (2 × 10^5/mL) were incubated with FITC-dextran (40 000 molecular weight; Sigma Chemical) or FITC-latex beads (2 μm; Polysciences, Warrington, PA) for 1 hour at 37°C or 4°C. The uptake of FITC-dextran and FITC-latex beads was halted by the addition of cold 1% FBS PBS. After washing 3 times with 1% FBS PBS, cells were analyzed on a FACS flow cytometer.[28,29]

Results

### CD15$^+$CD14$^-$ neutrophils generate macrophages

We isolated CD15$^+$CD14$^-$ cells from human blood samples. Portions of May-Grünwald-Giemsa–, MPO-, and double-specific/nonspecific esterase–stained preparations are presented in Figure 1A. The CD15$^+$CD14$^-$ cell fraction consisted of myelocytes, metamyelocytes, band cells, and segmented cells. Proportions of myelocytes, metamyelocytes, band cells, and segmented cells were 0.6% ± 0.2%, 9.2% ± 2.5%, 87.6% ± 2.5%, and 2.6% ± 0.4%, respectively (n = 5). CD15$^+$CD14$^-$ cells were positive for MPO and specific esterase but negative for nonspecific esterase. These staining patterns were found in all portions of cytospin preparations. We analyzed the cell cycle characteristics of CD15$^+$CD14$^-$ cells. All CD15$^+$CD14$^-$ cells were found in G$_1$ phase of the cell cycle (Figure 1B), supporting the notion that these cells are postmitotic. The expression of MPO, M-CSFR, lactoferrin, mannose receptor, and HLA-DR was assessed by phenotypic analysis (Figure 1C). CD15$^+$CD14$^-$ cells were MPO$^+$, M-CSFR$^-$, lactoferrin$^+$, mannose receptor$^-$, and HLA-DR$^-$, a finding compatible with typical features of mature neutrophils. CD14$^+$ cells were also prepared from blood samples. Cultures of CD14$^+$ cells in the presence of M-CSF gave rise to cells with small nuclei and intracytoplasmic vacuoles. These
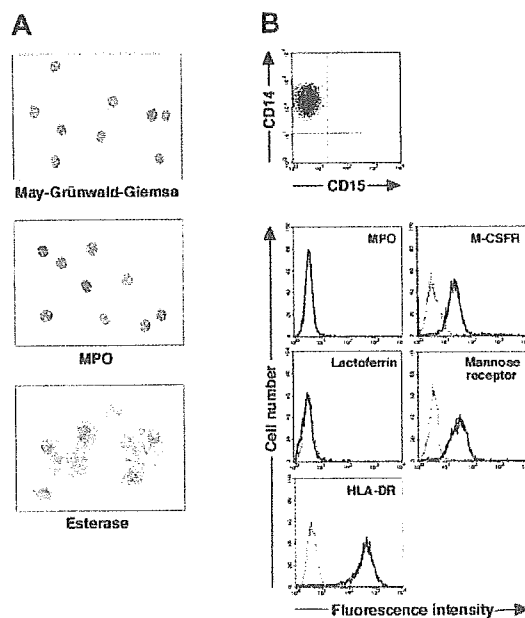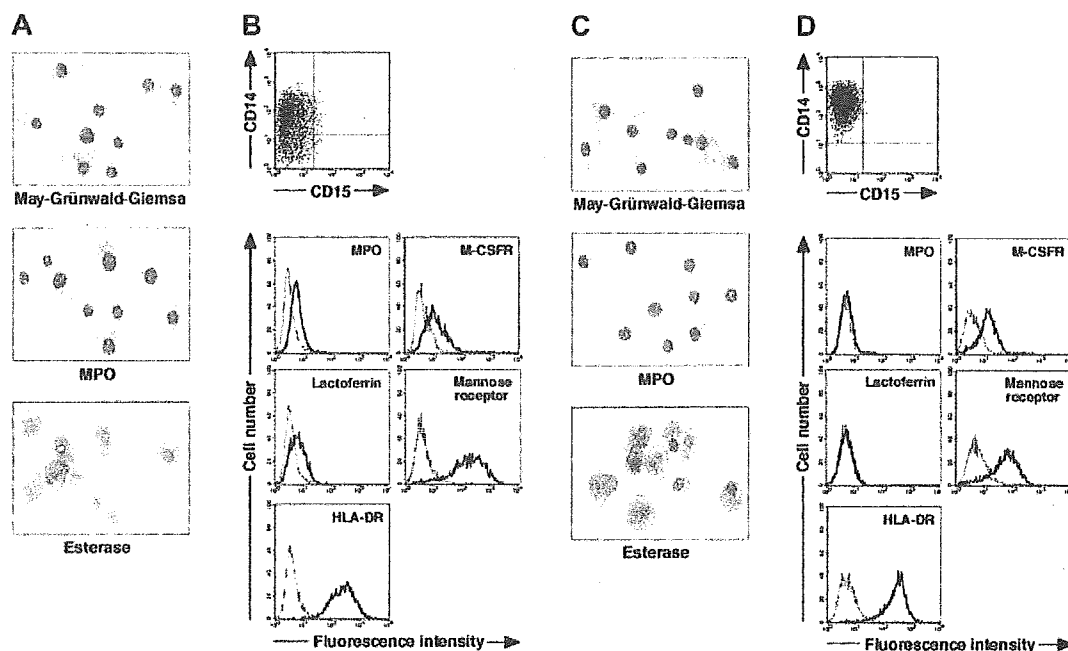

Figure 2. Cytochemistry and phenotype of cells obtained from 7-day culture of freshly isolated CD14$^+$ cells with M-CSF. (A) Photographs of May-Grünwald-Giemsa–, MPO-, and double specific/nonspecific esterase–stained cytospin preparations; original magnification, × 400. (B) The expression of CD15/CD14, MPO, M-CSFR, lactoferrin, mannose receptor, and HLA-DR was analyzed using a FACS-Calibur flow cytometer. In the histograms, the thick and thin lines show the expression of the indicated molecules and isotype controls, respectively. Yield of cultured cells was 52.8% ± 9.8% (n = 5). Representative data from 5 independent experiments are shown.

cells showed nonspecific esterase activity but not MPO or specific esterase activity (Figure 2A), and they exhibited the phenotype of CD15$^-$ CD14$^+$, MPO$^-$, M-CSFR $^+$, lactoferrin$^-$, mannose receptor$^+$, and HLA-DR$^+$ (Figure 2B), which suggested that the resultant cells were macrophages. CD15$^+$CD14$^-$ cells were also cultured in the presence of M-CSF for 7 days. The yield was less than 2% of the starting population. Surviving cells retained the features of neutrophils (data not shown).

To determine whether postmitotic neutrophils have the potential to alter the lineage, we attempted to drive CD15$^+$CD14$^-$ cells to become cells of a monocyte/macrophage lineage, using cultures supplemented with cytokines. The combination of GM-CSF, M-CSF, TNF-α, and IFN-γ was chosen because GM-CSF, M-CSF, TNF-α, and IFN-γ are known to favor the differentiation of monocytes and their progenitors into macrophages.[1,30-36] Because M-CSF is a cytokine specific for, and late-acting in, a monocyte/macrophage lineage, we cultured CD15$^+$CD14$^-$ cells in the presence of GM-CSF, TNF-α, and IFN-γ for 11 days and subsequently replated the cells in cultures with M-CSF alone. On day 18 after the initiation of culture, cultured cells were harvested and characterized in morphologic, cytochemical, and phenotypic analyses. These cells had macrophage morphology (Figure 3A). Their MPO or specific esterase activity was not detected using light microscopy; however, the nonspecific esterase reaction was positive. CD14 expression was induced in a substantial, although not the entire, population of the resultant cells, but CD15 expression was completely lost (Figure 3B). When compared with freshly isolated CD15$^+$CD14$^-$ cells, the resultant cells did not entirely down-regulate MPO and lactoferrin yet they considerably up-regulated M-CSFR, mannose receptor, and HLA-DR. This culture condition yielded 1.8% ± 0.6% (n = 5) of the starting CD15$^+$CD14$^-$ cell population. These data suggest that GM-CSF, TNF-α, IFN-γ, and M-CSF allow CD15$^+$CD14$^-$ cells to become macrophages.
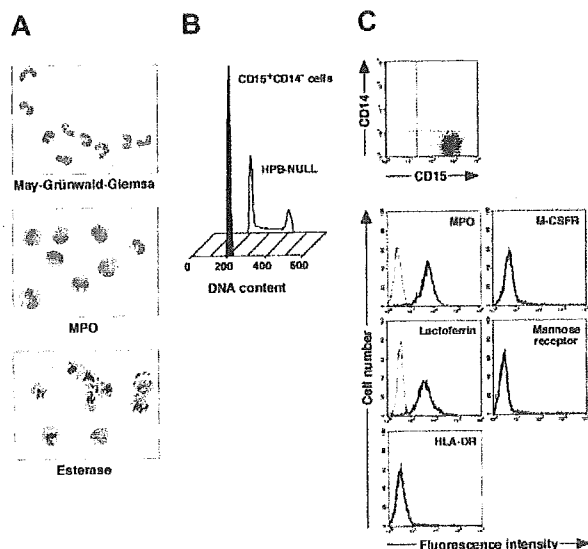
Figure 1. Cytochemistry and phenotype of freshly isolated CD15$^+$CD14$^-$ cells. (A) Photographs of May-Grünwald-Giemsa–, MPO-, and double-specific/nonspecific esterase–stained cytospin preparations; original magnification, × 400. (B) Nuclear DNA analysis of CD15$^+$CD14$^-$ cells was performed using a FACSCalibur flow cytometer. HPB-NULL cells were used as controls. Cell cycle distribution of HPB-NULL cells was as follows: with G$_1$ phase, 42.9%; S phase, 30.5%; and G$_2$/M phase, 26.6%. (C) The expression of CD15/CD14, MPO, M-CSFR, lactoferrin, mannose receptor, and HLA-DR was analyzed using a FACSCalibur flow cytometer. In the histograms, the thick and thin lines show the expression of the indicated molecules and isotype controls, respectively. Representative data from 5 independent experiments are shown.

Figure 3. Cytochemistry and phenotype of cells obtained from culture of freshly isolated CD15⁺CD14⁻ neutrophils. (A-B) Freshly isolated CD15⁺CD14⁻ neutrophils were cultured with GM-CSF, TNF-α, and IFN-γ for 11 days, followed by additional 7-day culture with M-CSF alone. (C-D) Freshly isolated CD15⁺CD14⁻ neutrophils were cultured with GM-CSF, TNF-α, IFN-γ, and IL-4 for 11 days, followed by additional 7-day culture with M-CSF alone. (A,C) Photographs of May-Grünwald-Giemsa-, MPO-, and double specific/nonspecific esterase–stained cytospin preparations; original magnification, × 400. (B,D) The expression of CD15/CD14, MPO, M-CSFR, lactoferrin, mannose receptor, and HLA-DR was analyzed using a FACSCalibur flow cytometer. In the histograms, the thick and thin lines show the expression of the indicated molecules and isotype controls, respectively. Representative data from 5 independent experiments are shown.

Next, we searched for cytokine(s). The addition of cytokines to cultures would allow cells derived from CD15⁺CD14⁻ cells to acquire features more typical of macrophages. After testing several cytokines, we found that the appropriate conditions could be satisfied by supplementation with IL-4. When cultured with GM-CSF, TNF-α, IFN-γ, and IL-4 for 11 days and with M-CSF alone for 7 days, CD15⁺CD14⁻ cells gave rise to cells with morphologic characteristics of macrophages. The resultant cells were negative for MPO and specific esterase activities and positive for nonspecific esterase activity on cytospin preparations (Figure 3C). Phenotypic analysis showed that the resultant cells lacked CD15 and exclusively expressed CD14. MPO and lactoferrin were completely down-regulated, whereas the high levels of M-CSFR, mannose receptor, and HLA-DR expression were retained (Figure 3D), as in the macrophage phenotype induced from CD14⁺ cells by M-CSF. Strikingly, the yield increased to 15.1% ± 3.6% (n = 5) of the starting CD15⁺CD14⁻ cell population. These observations unambiguously demonstrated a cytokine-induced lineage switch of postmitotic neutrophils to macrophages. We also cultured CD15⁺CD14⁻ cells in the presence of GM-CSF, TNF-α, IFN-γ, and IL-4 for 11 days and analyzed their phenotypes using flow cytometry. Cultured cells expressed neither CD15 nor CD14 (Figure 4A). MPO and lactoferrin were detected at low levels, whereas the expression levels of M-CSFR, mannose receptor, and HLA-DR were high (Figure 4B). These data suggest that the expression levels of molecules that characterize postmitotic neutrophils or macrophages are not simultaneously altered during this lineage switch program.

Gene expression profiles of CD15⁺CD14⁻ neutrophils and macrophages

Given that the combination of cytokines consisting of GM-CSF, TNF-α, IFN-γ, IL-4, and M-CSF allowed for the generation of macrophages from CD15⁺CD14⁻ neutrophils, as determined by morphologic, cytochemical, and phenotypic analyses, we com-

pared the gene expression profiles of freshly isolated CD15⁺CD14⁻ neutrophils, CD15⁺CD14⁻ neutrophil–derived macrophages, and CD14⁺ cell–derived macrophages using high-density oligonucleotide microarrays. Because every microarray was repeated twice, the mean expression intensity was calculated for each gene and was used for the following analysis. Among our expression data set, first searched were the genes expressed abundantly in CD15⁺CD14⁻ neutrophils but not in CD14⁺ cell–derived macrophages. Table 1 shows 10 such genes that had an expression level of more than 100 arbitrary units in CD15⁺CD14⁻ neutrophils and the highest ratio of the expression level between CD15⁺CD14⁻ neutrophils and CD14⁺
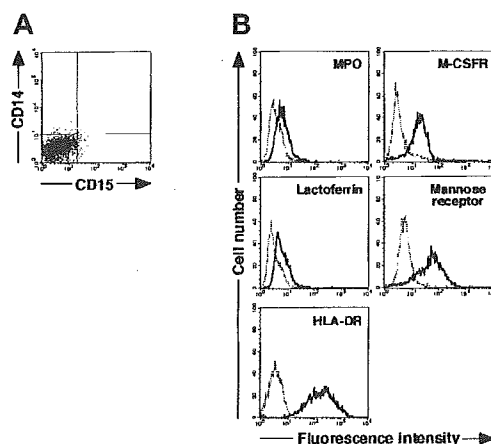
Figure 4. Cytochemistry and phenotype of cells obtained from culture of freshly isolated CD15⁺CD14⁻ neutrophils with GM-CSF, TNF-α, IFN-γ, and IL-4 for 11 days. (A) Expression pattern of CD15/CD14. (B) The expression of CD15/CD14, MPO, lactoferrin, M-CSFR, mannose receptor, and HLA-DR was analyzed using a FACSCalibur flow cytometer. In the histograms, the thick and thin lines show the expression of the indicated molecules and isotype controls, respectively. Representative data from 5 independent experiments are shown.

Table 1. Genes specifically expressed in CD15⁺CD14⁻ neutrophils

Gene symbol	GenBank accession no.	CD15⁺CD14⁻ neutrophil/ CD14⁺ cell-derived macrophage ratio	CD15⁺CD14⁻ neutrophils	CD14⁺ cell-derived macrophages	CD15⁺CD14⁻ neutrophil-derived macrophages
bA209J19.1	AL390736	5412.83	1623.85	0.30	0.60
LTF	NM_002343	2795.52	3773.95	1.35	1.50
DEFA3	NM_004084	1142.16	15 761.80	13.80	9.65
S100P	NM_005980	1099.67	3189.05	2.90	28.05
SGP28	NM_006061	699.78	314.90	0.45	0.45
CEACAM8	M33326	588.24	1323.55	2.25	3.30
LCN2	NM_005564	550.64	2945.90	5.35	8.90
DEFA4	NM_001925	499.83	2849.05	5.70	3.85
CD24	BG327863	474.81	759.70	1.60	8.75
FIZZ3	NM_020415	452.96	1223.00	2.70	5.90

Mean expression levels of genes in CD15⁺CD14⁻ neutrophils, CD14⁺ cell-derived macrophages, and CD15⁺CD14⁻ neutrophil-derived macrophages are shown in arbitrary units. The ratio between the first 2 is indicated in the CD15⁺CD14⁻ neutrophil/CD14⁺ cell-derived macrophage ratio.

cell-derived macrophages. Interestingly, all these CD15⁺CD14⁻ neutrophil-specific genes were also transcriptionally silent in CD15⁺CD14⁻ neutrophil-derived macrophages, as in CD14⁺ cell-derived macrophages. A well-known marker for granulocytes, CD24 (GenBank accession number AA761181) was only expressed in CD15⁺CD14⁻ neutrophils but not in CD15⁺CD14⁻ neutrophil-derived macrophages or CD14⁺ cell-derived macrophages. Conversely, we also tried to extract CD14⁺ cell-derived, macrophage-specific genes by comparing CD14⁺ cell-derived macrophages and CD15⁺CD14⁻ neutrophils (Table 2). Again, expression levels of these genes in the CD15⁺CD14⁻ neutrophil-derived macrophages were highly similar to those in CD14⁺ cell-derived macrophages. A monocyte/macrophage-specific cell surface antigen, CD163 (Z22969), was abundantly expressed in the CD15⁺CD14⁻ neutrophil-derived macrophages and the CD14⁺ cell-derived macrophages, but not in the CD15⁺CD14⁻ neutrophils. Hierarchical clustering analysis of these lineage-specific genes showed the similarity between gene expression profiles of CD15⁺CD14⁻ neutrophil-derived macrophages and CD14⁺ cell-derived macrophages (Figure 5A). Next, to statistically examine this similarity, we directly compared the 4 expression data sets of CD15⁺CD14⁻ neutrophils (n = 2) and CD14⁺ cell-derived macrophages (n = 2) and attempted to identify the genes, whose expression was different in the 2 groups (Welch ANOVA, $P < .001$). The expression profiles of such 9 lineage-dependent genes (Table 3) were then used to measure the similarity between CD14⁺ cell-derived macrophages and the other 2 groups. As shown in Figure 5B, 2-way clustering analysis[37] of 6 data sets (3 groups) clearly indicated that, with regard to gene expression profile, CD15⁺CD14⁻ neutrophil-derived macrophages were similar to

CD14⁺ cell-derived macrophages, separated from CD15⁺CD14⁻ neutrophils.

Phagocytic activity of CD15⁺CD14⁻ neutrophil-derived macrophages

Morphology, cytochemistry, phenotype, and gene expression of cultured cells in the presence of GM-CSF, TNF-α, IFN-γ, IL-4, and M-CSF indicated that CD15⁺CD14⁻ neutrophils became macrophages. Therefore, we next evaluated the phagocytic activity of these macrophages using FITC-dextran and FITC-latex beads. The potential for CD15⁺CD14⁻ neutrophil-derived macrophages to incorporate dextran and latex beads was comparable to that of CD14⁺ cell-derived macrophages (Figure 6).

Proliferative characteristics during culture

It is possible that macrophages induced from CD15⁺CD14⁻ neutrophils were derived from a small number of hematopoietic progenitor cells for macrophages that contaminated the CD15⁺CD14⁻ cell population and consequently proliferated. To exclude this possibility, we analyzed proliferative characteristics of the cultured cells; representative data are presented in Figure 7. In Figure 7A, the yield of cultured cells was 15.1%, on day 18 of culture. Reactivity with Ki-67 and incorporation of BrdU were tested on the indicated days of culture.[24,38] Ki-67⁺ or BrdU⁺ cells were not evident throughout the culture. Ki-67 expression and BrdU incorporation were observed most and approximately 30%, respectively, of HPB-NULL cells, which served as positive controls. We also used the carboxyfluorescein diacetate succinimidyl ester

Table 2. Genes specifically expressed in CD14⁺ cell-derived macrophages

Gene symbol	GenBank accession no.	CD14⁺ cell-derived macrophage/CD15⁺CD14⁻ neutrophil ratio	CD14⁺ cell-derived macrophages	CD15⁺CD14⁻ neutrophils	CD15⁺CD14⁻ neutrophil-derived macrophages
SEPP1	NM_005410	643.60	1769.90	2.75	1373.45
DAB2	NM_001343	307.52	1183.95	3.85	513.20
CD163	Z22969	256.43	2602.75	10.15	1034.35
ME1	NM_002395	197.02	551.65	2.80	310.10
CCL2	S69738	196.38	1708.50	8.70	351.10
ATP1B1	BC000006	180.35	775.50	4.30	408.85
FN1	BC005858	169.67	972.70	5.75	155.60
FN1	AK026737	162.44	1210.15	7.45	191.65
TGFBI	NM_000358	131.99	4045.55	30.65	3030.45
PMP22	L03203	129.14	1091.25	8.45	59.20

Mean expression levels of the genes in CD14⁺ cell-derived macrophages, CD15⁺CD14⁻ neutrophils, and CD15⁺CD14⁻ neutrophil-derived macrophages are shown in arbitrary units. The ratio between the first 2 is indicated in the CD14⁺ cell-derived macrophage/CD15⁺CD14⁻ neutrophil ratio.
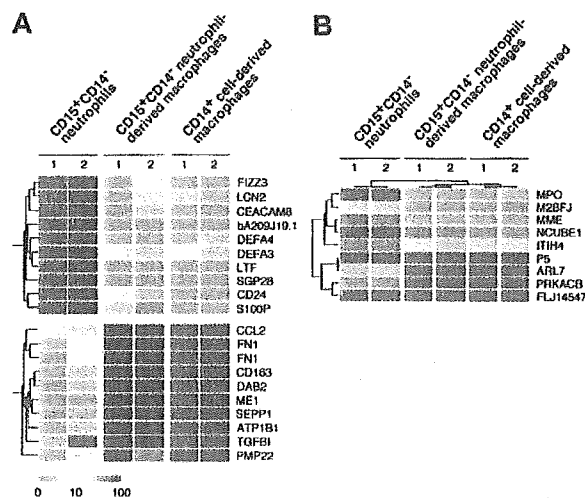
Figure 5. Expression profiles of neutrophil- and macrophage-specific genes. (A) Hierarchical clustering based on the expression intensities in CD15⁺CD14⁻ neutrophils, CD15⁺CD14⁻ neutrophil–derived macrophages, and CD14⁺ cell–derived macrophages was conducted for 10 genes with a specific expression in CD15⁺CD14⁻ neutrophils and CD14⁺ cell–derived macrophages (top panel) or in CD14⁺ cell–derived macrophages (bottom panel). Each row represents a single gene on the microarray, and each column represents a separate sample. Expression intensity of each gene is shown color coded, according to the scale at the bottom, and the gene symbols are indicated on the right. Expression data of these genes are available on request. (B) The gene tree was constructed using 2-way clustering analysis of the genes that are differentially (Welch ANOVA, P < .001) expressed between CD15⁺CD14⁻ neutrophils and CD14⁺ cell–derived macrophages. Each row represents a single gene on the microarray, and each column represents a separate sample. Expression intensity of each gene is shown color coded, according to the scale in panel A.

(CFSE) labeling technique to confirm that CD15⁺CD14⁻ neutrophils passed through no cell division during culture.[25] Analysis of the CFSE labeling pattern in CD8⁺ T cells, which had elicited several rounds of the cell cycle in response to CD3/CD28 T-cell expander beads, displayed a number of peaks of fluorescence (Figure 7B). However, the CFSE fluorescence remained a single peak in the cells generated by culturing CD15⁺CD14⁻ neutrophils with GM-CSF, TNF-α, IFN-γ, and IL-4 and subsequently with M-CSF alone. These data indicate that the generation of macrophages from the CD15⁺CD14⁻ cell population in culture is not associated with cell division.

Discussion

Lineage switch of normal primary cells has been noted in murine lymphoid progenitor cells.[21,22] Montecino-Rodriguez et al[21] ob-

Table 3. Genes with statistically different expression between CD15⁺CD14⁻ neutrophils and CD14⁺ cell-derived macrophages

Gene symbol	GenBank accession no.
MPO	J02694
H2BFJ	NM_003524
MME	NM_007287
NCUBE1	AF151039
ITIH4	D38535
P5	BC001312
ARL7	NM_005737
PRKACB	AA130247
FLJ14517	AV7113053

Gene symbols and GenBank accession numbers are shown for genes that exhibited significant differences in expression level between the 2 groups (Welch ANOVA, P < .001).
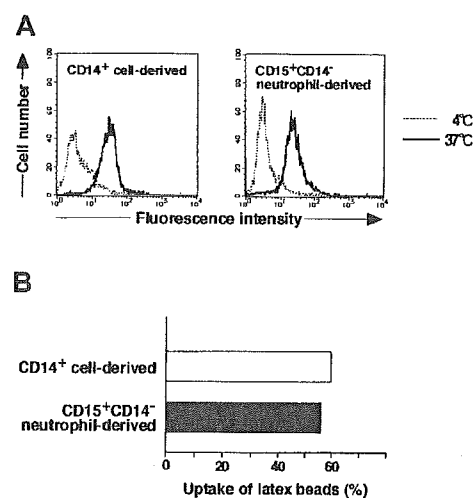
Figure 6. Phagocytic assay of CD15⁺CD14⁻ neutrophil–derived macrophages with FITC-dextran and FITC-latex beads. (A) CD15⁺CD14⁻ neutrophil– and CD14⁺ cell–derived macrophages were incubated with FITC-dextran for 1 hour at 37°C or 4°C, washed with cold PBS supplemented with 1% FBS, and analyzed using a FACSCalibur flow cytometer. Data are presented using histograms. (B) CD15⁺CD14⁻ neutrophil– and CD14⁺ cell–derived macrophages were incubated with FITC-latex beads for 1 hour at 37°C or 4°C, washed with cold PBS supplemented with 1% FBS, and analyzed with a FACSCalibur flow cytometer. Data are expressed as percentage of positive cells. Experiments were repeated 5 times with identical results.

served that a subpopulation of B-cell precursors in the bone marrow gave rise not only to B cells but also to macrophages in cultures supplemented with IL-3, IL-6, c-kit ligand, and GM-CSF. Lee et al[22] demonstrated that fetal thymocytes differentiate into
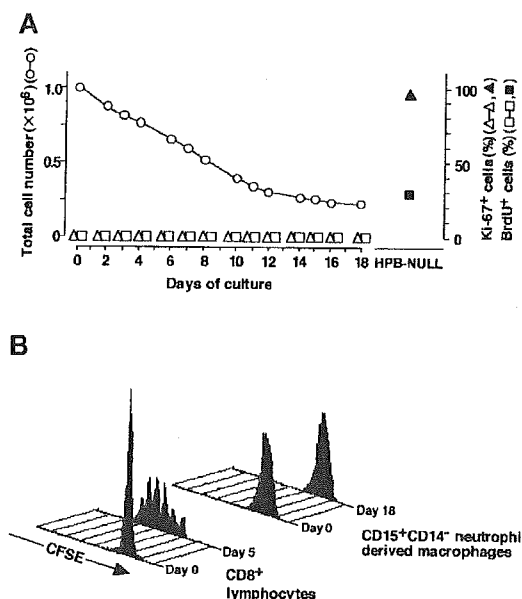
Figure 7. Analysis of proliferation profile. (A) CD15⁺CD14⁻ neutrophils were cultured with GM-CSF, TNF-α, IFN-γ, and IL-4 for 11 days, washed, and recultured with M-CSF alone for an additional 7 days. CD15⁺CD14⁻ neutrophils and the cultured cells were tested for Ki-67 staining and BrdU incorporation. Ki-67⁺ and BrdU⁺ cells were counted using a FACSCalibur flow cytometer, and the numbers were expressed as percentages. HPB-NULL cells were used as positive controls. Numbers of cultured cells are also indicated. Representative data from 5 independent experiments are shown. (B) CD15⁺CD14⁻ neutrophils were cultured with GM-CSF, TNF-α, IFN-γ, and IL-4 for 11 days, washed, and recultured with M-CSF alone for another 7 days. CD15⁺CD14⁻ neutrophils and the cultured cells were incubated with CFSE. Cell division patterns were analyzed using a FACSCalibur flow cytometer. CD8⁺ cells that underwent several rounds of the cell cycle in response to CD3/CD28 beads were used as positive controls. Experiments were repeated 5 times with identical results.

macrophages in the presence of M-CSF, IL-6, and IL-7 in vitro. A recent report stated that human B-cell progenitors obtained from cultures of cord blood CD34+CD10-CD19- cells gave rise to macrophages, NK cells, and T cells when exposed to the appropriate culture conditions.[23] Our study shows the lineage switch of human primary postnatal cells and further extends the existence of lineage switch to postmitotic cells. This notion is also supported by our observations in the microarray analysis that gene expression profiles of the resultant cells differed from those of the starting CD15+CD14- neutrophils and were similar to those of CD14+ cell–derived macrophages.

When we first cultured CD15+CD14- neutrophils in the presence of GM-CSF, TNF-α, IFN-γ, and M-CSF, the resultant cells displayed morphologic and cytochemical features of macrophages. However, they preserved a low level of MPO activity and lactoferrin expression, as determined by flow cytometry. These data suggest that the resultant cells did not fully exhibit the phenotypic characteristics of macrophages. Our surprise was that the addition of IL-4 to cultures was sufficient for the resultant cells to acquire typical features of macrophages. It is also of note that in the presence of IL-4, the yield of the resultant cells increased to approximately 15%. The phagocytic activity of macrophages generated in IL-4–containing cultures was of a similar magnitude compared with that observed with CD14+ cell–derived macrophages. Previous studies demonstrated the inhibitory activities of IL-4 on the development of monocytes/macrophages from progenitors supported by GM-CSF.[39,40] IL-4 has the potential to suppress TNF-α–induced effects on hematopoietic cells.[41] IL-4 also down-regulates the expression of 2 distinct receptors for TNF-α, p60, and p80 and induces shedding of these receptors, resulting in blockage of the cellular signaling elicited by TNF-α.[42] Moreover, several investigators have shown that IL-4 antagonizes IFN-γ–induced responses in human myeloid progenitor and mature cells.[43-45] Therefore, we have no plausible explanation for the mechanism of action of IL-4 on CD15+CD14- neutrophils during their lineage switch to macrophages. Complex networks by multiple cytokines may be involved in the generation of macrophages from CD15+CD14- neutrophils. Interestingly, phenotypic analysis indicated that when CD15+CD14- neutrophils turn their lineage toward macrophages, they lose CD15 expression and acquire CD14. This finding demonstrates that the down-regulation of CD15 occurs before the up-regulation of CD14. The cascade of several different events may lead to the lineage conversion of CD15+CD14- neutrophils to macrophages.

Our concern was whether a rare population of hematopoietic progenitors, contaminating the CD15+CD14- fraction, could proliferate and differentiate into macrophages. If such were the case,

the cultured cells would show signs of proliferation at several time points during culture. To address this issue, we used Ki-67 antibody staining, BrdU incorporation, and CFSE labeling. Neither Ki-67+ nor BrdU+ cells were detectable throughout culture, suggesting that cell division did not occur. In addition, if cultured cells had a history of successive cell divisions, we would have expected to observe separate peaks of CFSE fluorescence in the histogram. However, the narrow peak was observed with the resultant cells, as was the peak seen with the starting cell population. On the basis of these data and because the yield was approximately 15%, we assumed it was not possible for the cultured cells to have undergone more than one division throughout culture. Therefore, we propose that the generation of macrophages from CD15+CD14- neutrophils with GM-CSF, TNF-α, IFN-γ, IL-4, and M-CSF was not caused by contamination of progenitor cells for macrophages but was the result of their lineage switch to macrophages. It was also possible that a small number of monocyte/macrophage precursors contaminated the starting CD15+CD14- cell population. The yield in culture of CD15+CD14- cells with M-CSF and neutrophilic features of a marginal number of the surviving cells could conceivably exclude this possibility.

Our observation that postmitotic neutrophils could generate macrophages raises the issue of developmental origin of human macrophages and may represent another developmental pathway from hematopoietic stem cells toward macrophages. However, it is unclear whether such a neutrophil-to-macrophage lineage switch occurs under physiologic conditions. Such a lineage switch may occur under specified conditions, such as inflammation, because GM-CSF, TNF-α, IFN-γ, IL-4, and M-CSF are inflammatory cytokines. Oehler et al[46] demonstrate that neutrophil granulocyte-committed cells acquire dendritic cell features in the presence of GM-CSF, IL-4, and TNF-α. Our results indicated that when CD15+CD14- cells were cultured with GM-CSF, TNF-α, IFN-γ, and IL-4, the resultant cells exhibited a partial appearance of macrophages. IFN-γ may play a crucial role in the conversion of neutrophils into the macrophage lineage. In addition, it seems that neutrophils are capable of generating more types of mature cells than is generally recognized. Further studies on the reprogramming of already differentiated cells into other cell types are expected to yield new insights into events related to human hematopoiesis.

Acknowledgment

References

1. Metcalf D. The molecular control of cell division, differentiation commitment and maturation in haemopoietic cells. Nature. 1989;339:27-30.

2. Ogawa M. Differentiation and proliferation of hematopoietic stem cells. Blood. 1993;81:2844-2853.

3. Boyd AW, Schrader JW. Derivation of macrophagelike lines from the pre-B lymphoma ABLS 8.1 using 5-azacytidine. Nature. 1982;297:691-693.

4. Klinken SP, Alexander WS, Adams JM. Hemopoietic lineage switch: v-raf oncogene converts Eμ-myc transgenic B cells into macrophages. Cell. 1988;53:857-867.

5. Borzillo GV, Ashmun RA, Sherr CJ. Macrophage lineage switching of murine early pre-B lymphoid cells expressing transduced fms genes. Mol Cell Biol. 1990;10:2703-2714.

6. Lindeman G., Adams JM, Cory S, Harris AW. B-lymphoid to granulocytic switch during hematopoiesis in a transgenic mouse strain. Immunity. 1994;1:517-527.

7. Nutt SL, Heavey B, Rolink AG, Busslinger M. Commitment to the B-lymphoid lineage depends on the transcription factor Pax5. Nature. 1999;401:556-562.

8. Rolink AG, Nutt SL, Melchers F, Busslinger M. Long-term in vivo reconstitution of T-cell development by Pax5-deficient B-cell progenitors. Nature. 1999;401:603-606.

9. Kee BL, Murre C. Induction of early B cell factor (EBF) and multiple B lineage genes by the basic

helix-loop-helix transcriptional factor E12. J Exp Med. 1998;188:699-713.

10. Kondo M, Scherer DC, Miyamoto T, et al. Cell-fate conversion of lymphoid-committed progenitors by instructive actions of cytokines. Nature. 2000;407:383-386.

11. Iwasaki-Arai J, Iwasaki M, Miyamoto T, Watanabe S, Akashi K. Enforced granulocyte/macrophage colony-stimulating factor signals do not support lymphopoiesis, but instruct lymphoid to myelomonocytic lineage conversion. J Exp Med. 2003;197:1311-1322.

12. Iwasaki J, Mizuno S-I, Wells RA, Cantor AB, Watanabe S, Akashi K. GATA-1 converts lymphoid and myelomonocytic progenitors into the megakaryocyte/erythrocyte lineages. Immunity. 2003;19:451-462.

13. Visvader JE, Elefanty AG, Strasser A, Adams JM. GATA-1 but not SCL induces megakaryocytic differentiation in an early myeloid line. EMBO J. 1992;11:4557-4564.

14. Kulessa H, Frampton J, Graf T. GATA-1 reprograms avian myelomonocytic cell lines into eosinophils, thromboblasts, and erythroblasts. Genes Dev. 1995;9:1250-1262.

15. Seshasayee D, Gaines P, Wojchowski DM. GATA-1 dominantly activates a program of erythroid gene expression in factor-dependent myeloid FDCW2 cells. Mol Cell Biol. 1998;18:3278-3288.

16. Yamaguchi Y, Zon LI, Ackeman SJ, Yamamoto M, Suda T. Forced GATA-1 expression in the murine myeloid cell line M1: induction of c-Mpl expression and megakaryocytic/erythroid differentiation. Blood. 1998;91:450-457.

17. Yamada T, Kihara-Negishi F, Yamamoto H, Yamamoto M, Hashimoto Y, Oikawa T. Reduction of DNA binding activity of the GATA-1 transcriptional factor in the apoptotic process induced by overexpression of PU.1 in murine erythroleukemia cells. Exp Cell Res. 1998;245:186-194.

18. Muller C, Kowenz-Leutz E, Grieser-Ade S, Graf T, Leutz A. NF-M (chicken C/EBPβ) induces eosinophilic differentiation and apoptosis in a hematopoietic progenitor cell line. EMBO J. 1995;14:6127-6135.

19. Nerlov C, McNagny KM, Döderlein G, Kowenz-Leutz E, Graf T. Distinct C/EBP functions are required for eosinophilic lineage commitment and maturation. Genes Dev. 1998;12:2413-2423.

20. Querfurth E, Schuster M, Kulessa H, et al. Antagonism between C/EBPβ and FOG in eosinophil lineage commitment of multipotent hematopoietic progenitors. Genes Dev. 2000;14:2515-2525.

21. Montecino-Rodriguez E, Leathers H, Dorshkind K. Bipotential B-macrophages progenitors are present in adult bone marrow. Nat Immunol. 2001;2:83-88.

22. Lee C-K, Kim JK, Kim Y, et al. Generation of macrophages from early T progenitors in vitro. J Immunol. 2001;166:5964-5969.

23. Reynaud D, Lefort N, Manie E, Coulombel L, Levy Y. In vitro identification of human pro-B cells that give rise to macrophages, natural killer cells, and T cells. Blood. 2003;101:4313-4321.

24. Mahmud N, Katayama N, Nishii K, et al. Possible involvement of bcl-2 in regulation of cell-cycle progression in haemopoietic cells by transforming growth factor-β1. Br J Haematol. 1999;105:470-477.

25. Kovacs B, Maus MV, Riley JL, et al. Human CD8+ T cells do not require the polarization of lipid rafts for activation and proliferation. Proc Natl Acad Sci U S A. 2002;99:15006-15011.

26. Ohmine K, Ota J, Ueda M, et al. Characterization of stage progression in chronic myeloid leukemia by DNA microarray with purified hematopoietic stem cells. Oncogene. 2001;20:8249-8257.

27. Makishima H, Ishida F, Ito T, et al. DNA microarray analysis of T cell-type lymphoproliferative disease of granular lymphocytes. Br J Haematol. 2002;118:462-469.

28. Araki H, Katayama N, Mitani H, et al. Efficient ex vivo generation of dendritic cells from CD14+ blood monocytes in the presence of human serum albumin for use in clinical vaccine trials. Br J Haematol. 2001;114:681-689.

29. Oda T, Maeda H. A new simple fluorometric assay for phagocytosis. J Immunol Methods. 1986;88:175-183.

30. Metcalf D. Control of granulocytes and macrophages: molecular, cellular, and clinical aspects. Science. 1991;254:529-533.

31. Motoyoshi K. Biological activities and clinical application of M-CSF. Int J Hematol. 1997;67:109-122.

32. Witsell AL, Schook LB. Tumor necrosis factor α is an autocrine growth regulator during macrophage differentiation. Proc Natl Acad Sci U S A. 1992;89:4754-4758.

33. Tracey KJ, Cerami A. Tumor necrosis factor: a pleiotropic cytokine and therapeutic target. Annu Rev Med. 1994;45:491-503.

34. Friedman RM, Vogel SN. Interferons with special emphasis on the immune system. Adv Immunol. 1983;34:97-140.

35. Trinchieri G, Perussia B. Immune interferon: a pleiotropic lymphokine with multiple effects. Immunol Today. 1985;6:131-136.

36. Schreiber RD, Celada A. Molecular characterization of interferon γ as a macrophage activating factor. Lymphokines. 1985;11:87-118.

37. Alon U, Barkai N, Notterman DA, et al. Broad patterns of gene expression revealed by clustering analysis of tumor and normal colon tissues probed by oligonucleotides arrays. Proc Natl Acad Sci U S A. 1999;96:6745-6750.

38. Brons PPT, Raemaekers JMM, Bogman JJT, et al. Cell cycle kinetics in malignant lymphoma studied with in vivo iododeoxyuridine administration, nuclear Ki-67 staining, and flow cytometry. Blood. 1992;80:2336-2343.

39. Jansen JH, Wientjens G-JHM, Fibbe WE, Willemze R, Kluin-Nelemans HC. Inhibition of human macrophage colony formation by interleukin 4. J Exp Med. 1989;170:577-582.

40. Snoeck H-W, Lardon F, Van Bockstaeie DR, Peetermans ME. Effects of interleukin-4 (IL4) on myelopoiesis: studies on highly purified CD34+ hematopoietic progenitor cells. Leukemia. 1993;7:625-629.

41. Levesque MC, Haynes BF. Cytokine induction of the ability of human monocyte CD44 to bind hyaluronan is mediated primarily by TNF-α and inhibited by IL-4 and IL-13. J Immunol. 1997;159:6184-6194.

42. Manna SK, Aggarwal BB. Interleukin-4 downregulates both forms of tumor necrosis factor receptor and receptor-mediated apoptosis, NF-κB, AP-1, and c-Jun N-terminal kinase. J Biol Chem. 1998;273:33333-33341.

43. te Velde AA, Huijbens RJF, de Vries JE, Figdor CG. IL-4 decreases FcγR membrane expression and FcγR-mediated cytotoxic activity of human monocytes. J Immunol. 1990;144:3046-3051.

44. te Velde AA, Huijbens RJF, Heije K, de Vries JE, Figdor CG. Interleukin-4 (IL-4) inhibits secretion of IL-1β, tumor necrosis factor α, and IL-6 by human monocytes. Blood. 1990;76:1392-1397.

45. Snoeck H-W, Lardon F, Lenjou M, Nys G, Van Bockstaele DR, Peetermans ME. Interferon-γ and interleukin-4 reciprocally regulate the production of monocytes/macrophages and neutrophils through a direct effect on committed monopotential bone marrow progenitor cells. Eur J Immunol. 1993;23:1072-1077.

46. Oehler L, Majdic O, Pickl WF, et al. Neutrophil granulocyte-committed cells can be driven to acquire dendritic cell characteristics. J Exp Med. 1998;187:1019-1028.

Mutual Regulation of Protein-tyrosine Phosphatase 20 and Protein-tyrosine Kinase Tec Activities by Tyrosine Phosphorylation and Dephosphorylation*

Naohito Aoki‡§, Shuichi Ueno¶, Hiroyuki Mano¶, Sho Yamasaki‖, Masayuki Shiota**,
Hitoshi Miyazaki**, Yumiko Yamaguchi-Aoki‡‡, Tsukasa Matsuda‡, and Axel Ullrich‡‡

From the ‡Department of Applied Molecular Biosciences, Graduate School of Bioagricultural Sciences, Nagoya University,
Furo-cho, Chikusa-ku, Nagoya 464-8601, Japan, ¶Divisions of Functional Genomics, Cardiology and Hematology,
Jichi Medical School, Kawachi-gun, Tochigi 329-0498, Japan, ‖Molecular Genetics, Chiba University Graduate
School of Medicine, Chiba 260-8670, Japan, **Gene Research Center, University of Tsukuba, Ibaraki 305-8572, Japan,
and ‡‡Max Planck Institute for Biochemistry, Department of Molecular Biology, D-82152 Martinsried, Germany

PTP20, also known as HSCF/protein-tyrosine phosphatase K1/fetal liver phosphatase 1/brain-derived phosphatase 1, is a cytosolic protein-tyrosine phosphatase with currently unknown biological relevance. We have identified that the nonreceptor protein-tyrosine kinase Tec-phosphorylated PTP20 on tyrosines and co-immunoprecipitated with the phosphatase in a phosphotyrosine-dependent manner. The interaction between the two proteins involved the Tec SH2 domain and the C-terminal tyrosine residues Tyr-281, Tyr-303, Tyr-354, and Tyr-381 of PTP20, which were also necessary for tyrosine phosphorylation/dephosphorylation. Association between endogenous PTP20 and Tec was also tyrosine phosphorylation-dependent in the immature B cell line Ramos. Finally, the Tyr-281 residue of PTP20 was shown to be critical for deactivating Tec in Ramos cells upon B cell receptor ligation as well as dephosphorylation and deactivation of Tec and PTP20 itself in transfected COS7 cells. Taken together, PTP20 appears to play a negative role in Tec-mediated signaling, and Tec-PTP20 interaction might represent a negative feedback mechanism.

Protein-tyrosine phosphatases (PTPs)[1] are a large and structurally diverse family of enzymes that catalyze the dephosphorylation of tyrosine-phosphorylated proteins (1, 2). Biochemical and kinetic studies have documented that Cys and an Asp residues in the catalytic domain are essential for the PTP activity. PTPs have been shown to participate as either positive or negative regulators of signaling pathways in a wide range of physiological processes, including cellular growth, differentiation, migration, and survival (1, 2). Despite their important roles in such fundamental cellular processes, the mechanisms by which PTPs exert their effects are largely not understood.

PTP20 (3), which is also known as hematopoietic stem cell fraction (HSCF) (4), PTP-K1 (5), fetal liver phosphatase 1 (6), and brain-derived phosphatase 1 (7), comprises the PEST family of PTPs together with PTP-PEST and PEP PTP and was originally isolated by screening a PC12 cDNA library. Overexpression of PTP20 in PC12 cells results in a more rapid and robust neurite outgrowth in response to nerve growth factor treatment, suggesting that PTP20 is involved in cytoskeletal reorganization (3). Mostly consistent with this observation, overexpression of a dominant negative mutant of fetal liver phosphatase 1 in K562 hematopoietic progenitor cells results in an inhibition of cell spreading and substrate adhesion in response to phorbol ester (6). Recently, through yeast two-hybrid screening the proline, serine, threonine phosphatase-interacting protein (PSTPIP) and PSTPIP2 have been identified to be specific in vivo substrates for HSCF, because the phosphotyrosine (Tyr(P)) level of PSTPIP1 is significantly enhanced by coexpression of the catalytically inactive mutant (Cys to Ser) of PTP20 (8, 9). PSTPIP is tyrosine-phosphorylated both in BaF3 cells and in v-Src-transfected COS cells and is shown to be co-localized with the cortical actin cytoskeleton, lamellipodia, and actin-rich cytokinetic cleavage furrow (8), strongly supporting the idea that PTP20/HSCF is a potential regulator of cytokinesis. PSTPIP also interacts with the C-terminal part of the cytosolic protein-tyrosine kinase (PTK) c-Abl, serves as a substrate for c-Abl, and can bridge interactions between c-Abl and PTP20 with the dephosphorylation of c-Abl by PTP20 (10). It has also been reported that PTP20 associates with the negative Src-family kinase regulator Csk via its Src homology 2 (SH2) domain and two putative sites of tyrosine phosphorylation of the phosphatase (11). This association is thought to allow Csk and PTP20 to synergistically inhibit Src-family kinase activity by phosphorylating and dephosphorylating negative and positive regulatory tyrosine residues, respectively.

Regarding post-translational regulation of the PEST family PTPs, it has been documented that phosphorylation of an N-terminal serine residue, which is well conserved in all members of the PEST PTP family, by protein kinase A results in the inhibition of its catalytic activity (12). In addition to proline, serine, and threonine residues in the C-terminal PEST domain of PTP20, a large number of tyrosine residues exist in that region, suggesting the possibility that PTP20 is tyrosine-phosphorylated. Indeed, previous studies reveal that PTP20/HSCF

§ To whom all correspondence should be addressed: Dept. of Applied Molecular Biosciences, Graduate School of Bioagricultural Sciences, Nagoya University, Furo-cho, Chikusa-ku, Nagoya 464-8601, Japan. Fax: 81-52-789-4128; E-mail: naoki@agr.nagoya-u.ac.jp.

[1] The abbreviations used are: PTP, protein-tyrosine phosphatase; HSCF, hematopoietic stem cell fraction; PSTPIP, proline, serine, threonine phosphatase-interacting protein; PTK, protein-tyrosine kinase; BCR, B cell receptor; SH2, Src homology 2; SH3, Src homology 3; HA, hemagglutinin; GST, glutathione S-transferase; WT, wild type; ECL, enhanced chemiluminescence; PH, pleckstrin homology; TH, Tec homology; POV, pervanadate.

becomes tyrosine-phosphorylated by constitutively active forms of Lck and v-Src kinases in transfected cells (8, 11) even though the physiological relevance of tyrosine phosphorylation on PTP20 remains unclear.

In this study we addressed the question of PTP20 regulation with special emphasis on the relevance of tyrosine phosphorylation and its biological impact. Through co-expression with nonreceptor PTKs we found that Tec kinase strongly tyrosine-phosphorylated the catalytically inactive form of PTP20 and that Tec physically interacted with PTP20 in a tyrosine phosphorylation-dependent manner in transfected COS7 cells. Further analyses with a variety of mutants of PTP20 and Tec revealed that C-terminal tyrosine residues of PTP20 and the Tec SH2 domain were necessary in the regulation of respective state of phosphorylation. Ectopic expression of PTP20 in human immature Ramos B cells resulted in suppression of B-cell receptor-induced c-*fos* promoter activity. Moreover, we determined that tyrosine 281 of PTP20 played a role in the dephosphorylation activity of PTP20 against both Tec and PTP20 itself. Our findings suggest a negative feedback mechanism that mutually controls the tyrosine phosphorylation of Tec and PTP20 and regulates Tec activity and B cell receptor (BCR) signaling.

EXPERIMENTAL PROCEDURES

Reagents—Antibodies to hemagglutinin (HA) epitope (Y-11), phosphotyrosine (PY99), glutathione S-transferase (GST) (Z-5), Src (SRC2), Lck (2102), JAK2 (M-126), JAK3 (C-21), Csk (C-20), and ZAP70 (LR) were purchased from Santa Cruz Biotechnology Inc. (Santa Cruz, CA). Antibodies to Tec, Itk, Btk, and Bmx were as described previously (13). Antibody to PTP20 was prepared by immunizing rabbits with the N-terminal peptide of PTP20 (MSRQSDLVRSFLEQQEARDH), to which a cysteine residue was added to the C terminus, coupled to keyhole limpet hemocyanin (14). Anti-human IgM antibody (Fab')$_2$ fragment was obtained from Southern Biotechnology Associates (Birmingham, AL). All other reagents were from Sigma unless otherwise noted.

Plasmid Construction—The pSR-based expression vectors for Tec wild-type (WT), Tec kinase mutant, TecY187F, TecY518F, and Tec proteins lacking each subdomain were described previously (15, 16). pEBG plasmids (17) encoding each subdomain of Tec to express the GST-tagged proteins were previously described (18). HA epitope tagging to PTP20 at its N terminus and subsequently all the mutations (cysteine to serine, aspartic acid to alanine, and tyrosine to phenylalanine) in PTP20 were carried out by PCR-based strategy. To express GST-tagged PTP20 in mammalian cells, full-length PTP20 (amino acids 2–453), PTP catalytic domain (amino acids 2–308), and the C-terminal noncatalytic PEST domain (amino acids 271–453) were amplified by PCR and ligated into pEBG vector via the BamHI site. All the plasmids newly constructed were confirmed by sequencing. Expression plasmids for rat Csk and mouse JAK2 were generous gifts from Drs. M. Okada (Osaka University, Japan) and J. N. Ihle (St. Jude Children's Research Hospital, Memphis, TN), respectively. Expression plasmids for mouse Src, Lck, Itk, Btk, Bmx, ZAP-70, and JAK3 were described elsewhere.

Cell Culture and Transfection—COS7 cells were cultured in Dulbecco's modified Eagle's medium (high glucose, Sigma) supplemented with 10% fetal calf serum. Ramos cells (American Type Culture Collection, Manassas, VA) were maintained in RPMI 1640 medium (Invitrogen) supplemented with 10% fetal calf serum. Upon transfection experiments COS7 cells were inoculated at a density of 4×10^5 cells/6-cm dish and grown overnight in Dulbecco's modified Eagle's medium containing 10% fetal calf serum. Expression plasmids were transfected into the cells by the modified calcium phosphate precipitation method (19). After incubation under 3% CO_2, 97% air for 18 h, the transfected cells were washed with phosphate-buffered saline twice and cultured in fresh Dulbecco's modified Eagle's medium containing 10% fetal calf serum for another 24 h under humidified 5% CO_2 and 95% air.

Cell Lysis, Immunoprecipitation, GST Pull-down, and Western Blotting—The transfected cells were lysed with lysis buffer containing 50 mM Tris-HCl (pH 7.5), 5 mM EDTA, 150 mM NaCl, 10 mM sodium phosphate, 10 mM sodium fluoride, 1% Triton X-100, 1 mM phenylmethylsulfonyl fluoride, and 10 μg/ml leupeptin. Lysates were directly subjected to immunoblotting, immunoprecipitation with the indicated antibodies plus protein G- or Protein A-Sepharose beads (Amersham Bioscience), or precipitation with GSH-Sepharose beads (Amersham

Bioscience). Proteins in the immunoprecipitates and precipitates were further analyzed by immunoblotting with the indicated antibodies. The protein bands were visualized with an enhanced chemiluminescence (ECL) detection kit (Amersham Bioscience) and light capture system (AE-6962, ATTO, Tokyo, Japan).

c-fos Promoter Assay—Ramos cells (1×10^7/experiment) were subjected to electroporation with 2 μg of the pfos/luc reporter plasmid (20) plus 10 μg of expression plasmids for PTP20 or its mutants. Five hours after transfection cells were incubated for 5 h in the absence or presence of antibodies to human IgM (10 μg/ml). Luciferase activity was measured with the use of the dual luciferase assay system (Promega, Madison, WI).

RESULTS

Tec Is a Potent Regulator of PTP20—Although PTP20 has been shown to be a substrate of v-Src (8) and constitutively active Lck (11), the physiological relevance of PTP20 tyrosine phosphorylation remains unknown. Northern blot analysis revealed that PTP20 was abundantly expressed in spleen, suggesting a role in the immune system (data not shown). Therefore, it was reasoned that other PTKs of immune cells might be involved in PTP20 regulation by tyrosine phosphorylation. To examine this possibility HA-tagged PTP20 was co-expressed with various cytosolic PTKs including Src and Lck in COS7 cells. We used a catalytically inactive form of PTP20 for this experiment because autodephosphorylation activity of PTP20 has been previously reported (8). Cells were lysed, PTP20 was immunoprecipitated with anti-HA antibody, and the immune complexes were subjected to SDS-PAGE and immunoblotting with anti-phosphotyrosine antibody. As shown in Fig. 1A, PTP20 was tyrosine-phosphorylated by Src and Lck and co-immunoprecipitated with proteins with 56 and 60 kDa, likely corresponding to Lck and Src, respectively. In the case of ectopic Lck expression, endogenous Src seemed to be included in the immune complex, as suggested by the presence of a 66-kDa phosphotyrosine-containing band. PTP20 was slightly tyrosine-phosphorylated by Csk and co-immunoprecipitated with a faintly tyrosine-phosphorylated 70-kDa band, which seemed unlikely to be Csk. JAK2 but not JAK3 also tyrosine-phosphorylated PTP20 and appeared to be co-immunoprecipitated with PTP20. Most notably, PTP20 was strongly tyrosine-phosphorylated by Tec and co-immunoprecipitated with a heavily tyrosine-phosphorylated protein of 74 kDa and other minor proteins of 120 and 35 kDa. Based on the molecular mass, the 74-kDa protein was likely to represent Tec. Itk, another member of Tec/Btk family, also tyrosine-phosphorylated PTP20 to a lesser extent and was co-immunoprecipitated, whereas related PTKs Btk and Bmx did not tyrosine phosphorylate PTP20 and were not co-immunoprecipitated. Because all the transfected PTKs were obviously expressed as compared with mock transfectant (Fig. 1, *panel B*), it was suggested that Tec tyrosine-phosphorylated PTP20 with the greatest efficiency.

Tec Is a Potential Substrate of PTP20—To examine the relationship between PTP20 and Tec in more detail, Tec was co-transfected with WT or a catalytically inactive C/S form of PTP20 into COS7 cells, and either PTP20 or Tec was immunoprecipitated followed by immunoblotting with anti-phosphotyrosine antibody. When HA-PTP20 WT was expressed, no phosphorylated bands were visible in both anti-HA and anti-Tec immunoprecipitates, possibly due to dephosphorylation activity of PTP20 against both Tec and itself (Fig. 2). Two major bands with 74 and 50 kDa in the anti-HA and anti-Tec immune complexes were detected with anti-phosphotyrosine antibody only when the PTP20 C/S mutant was co-transfected with Tec. Reprobing with anti-Tec and anti-HA antibodies clearly revealed that the bands represent Tec and HA-PTP20. No phosphorylation of Tec was observed when Tec alone was introduced into COS7 cells, suggesting that the interaction between Tec and PTP20 was required for Tec phosphorylation and pos-

A

B
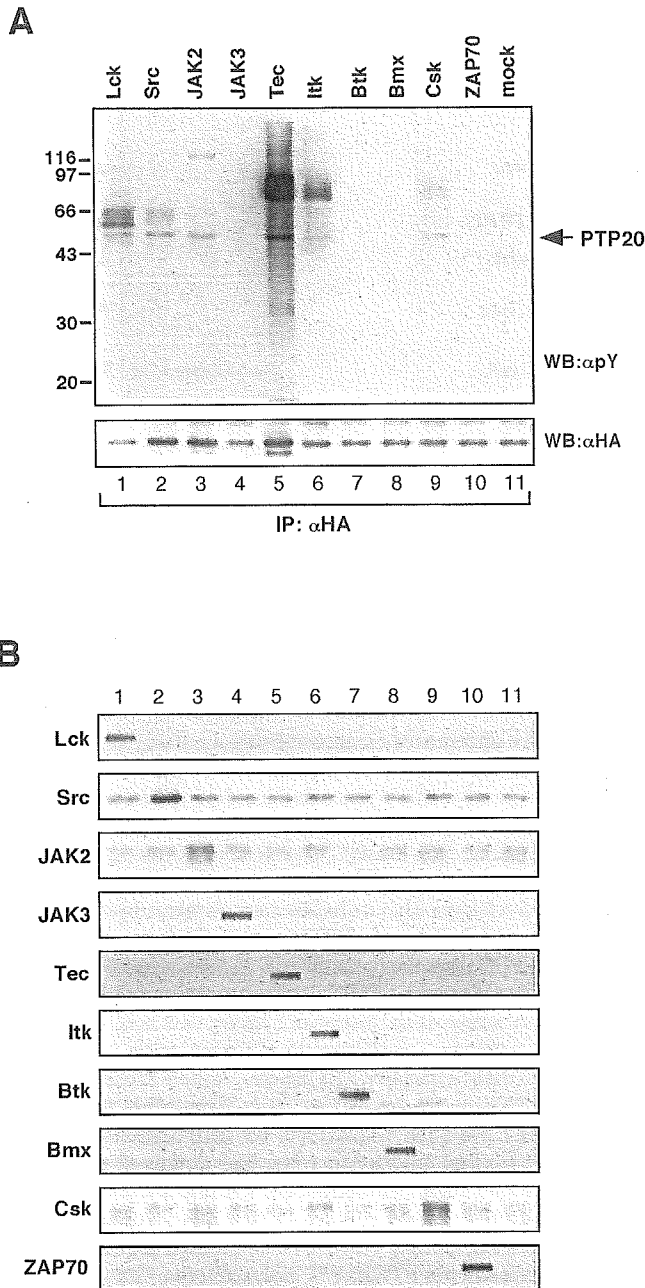
FIG. 1. **Tyrosine phosphorylation of PTP20 by various PTKs.** *A*, COS7 cells were transiently transfected with HA-PTP20 C/S together with either Lck, Src, JAK2, JAK3, Tec, Itk, Btk, Bmx, Csk, or ZAP70. Cells were lysed, and PTP20 was immunoprecipitated (*IP*) with anti-HA antibody followed by immunoblotting (*WB*) with anti-phosphotyrosine antibody (PY99 (*αpY*)). The same membrane was reprobed with anti-HA antibody after stripping. *B*, an aliquot of the cell lysates was immunoblotted with the indicated antibodies to confirm substantial expression of each PTK.

sibly activation. These results suggest that PTP20 is a substrate of Tec and that Tec is also a substrate of PTP20.

Phosphotyrosine-dependent Interaction between PTP20 and Tec—Tec is composed of several distinct domains including pleckstrin homology (*PH*), Tec homology (*TH*), SH3, SH2, and kinase (*KD*) domains (Fig. 3, *panel A*). All of these domains are necessary for full function of Tec under physiological conditions (15, 16). To examine which domains are involved in interaction with PTP20, Tec mutants each lacking one of the domains were co-transfected with the catalytically inactive form of PTP20 into COS7 cells. A kinase mutant as well as two mutants (Y187F and Y518F) where tyrosine residues were replaced by

phenylalanines were also included. Cells were lysed, and PTP20 was immunoprecipitated followed by immunoblotting with anti-phosphotyrosine antibody. PTP20 was tyrosine-phosphorylated by the Y187F mutant as well as mutants lacking PH, TH, and SH3 domains to a similar extent as compared with Tec WT (Fig. 3, *panel B*). As expected, the Y518F mutant, which is missing the autophosphorylation site for Tec activation, and the inactive mutant of a kinase mutant could not tyrosine phosphorylate PTP20. Interestingly, the ΔPH mutant could tyrosine phosphorylate PTP20 but was not co-immunoprecipitated with PTP20. Most strikingly, the ΔSH2 mutant could not tyrosine phosphorylate PTP20 and was not co-immunoprecipitated with PTP20. When a membrane on which aliquots of total cell lysates were blotted was probed with anti-phosphotyrosine antibody, it was revealed that co-expression of the Tec ΔSH2 mutant and PTP20 resulted in no tyrosine phosphorylation on both molecules and that the Tec ΔPH mutant tyrosine-phosphorylated (Fig. 3, *panel C*). Tec SH2 domain-dependent interaction with PTP20 was further investigated by co-transfecting the PTP20 C/S mutant with plasmids encoding GST fusion proteins of Tec domains in the presence or absence of Tec into COS7 cells. Cell lysates were subjected to pull-down experiments with GSH-Sepharose beads. Precipitates were separated by SDS-PAGE followed by immunoblotting with the indicated antibodies. In the absence of full-length Tec co-expression, no substantial binding of PTP20 to any of the Tec domains was apparent (Fig. 3, *panel D*). In contrast, in the presence of full-length Tec, phosphorylated PTP20 bound to only the SH2 domain of Tec. Given that co-expression of Tec should result in marked tyrosine phosphorylation of PTP20 in COS7 cells, these data indicate that the PTP20-Tec interaction is mediated predominantly by the SH2 domain of Tec and phosphotyrosine residues of PTP20.

Next, we tried to identify the binding site(s) for Tec in PTP20. Because the interaction of Tec with PTP20 was mediated by the Tec SH2 domain, potential tyrosine residues of phosphorylation were first taken into consideration. There are 13 tyrosine residues (Tyr-62, Tyr-68, Tyr-86, Tyr-101, Tyr-144, Tyr-192, Tyr-244, Tyr-281, Tyr-285, Tyr-303, Tyr-354, Tyr-381, Tyr-419) in the PTP20 sequence, and all the residues are perfectly conserved among human and mouse orthologs (Fig. 4). We focused our attention on the tyrosine residues Tyr-281, Tyr-285, Tyr-303, Tyr-354, Tyr-381, and Tyr-419 located in the C-terminal PEST domain of PTP20, and 6 residues were individually mutated.

First, the mutants were tested for the extent of tyrosine phosphorylation by Tec in transfected COS7 cells. Total cell lysates were subjected to anti-phosphotyrosine blotting. Fig. 5, *panel A*, demonstrates that the PTP20 mutants (Y281F, Y303F, Y354F, Y381F) in which Tyr-281, Tyr-303, Tyr-354, and Tyr-381 were individually mutated exhibited dramatic reduction in tyrosine phosphorylation levels, whereas no apparent reduction for Y285F and Y419F was observed. Combinational mutation of Tyr-281, Tyr-303, Tyr-354, and Tyr-381 totally abolished tyrosine phosphorylation of PTP20. In keeping with these data, anti-phosphotyrosine blotting also demonstrated that tyrosine phosphorylation of Tec was concomitantly reduced. This observation was further extended by GST pull-down experiments using the Tec SH2 domain. COS7 cells were then transfected with PTP20 YF variants together with Tec and Tec-Tec SH2, as outlined in Fig. 3, *panel C*. Mutation of either Tyr-281, Tyr-303, Tyr-354, or Tyr-381 of PTP20 resulted in reduced binding capacity of PTP20 to the Tec SH2 domain, and again, such binding was completely abrogated by substituting all the tyrosine residues (Fig. 5, *panel B*). Together these data clearly indicate that four tyrosine residues in the C-ter-

FIG. 2. **Tyrosine phosphorylation-dependent interaction of PTP20 with Tec.** Tec cDNA was transiently introduced into COS7 cells together with either empty vector (mock), HA-PTP20 WT, or C/S and lysed. PTP20 or Tec was immunoprecipitated either with anti-HA (*left panels*) or anti-Tec (*right panels*) antibody, respectively. The immunoprecipitates (*IP*) were separated by SDS-PAGE followed by immunoblotting (*WB*) sequentially with the indicated antibodies. The bands corresponding to Tec and PTP20 are indicated by *arrows*. In either case expression of Tec or HA-PTP20 was confirmed using aliquots of total cell lysates (*TCL*) by immunoblotting (*lowest panels*). αpY, anti-phosphotyrosine antibody.
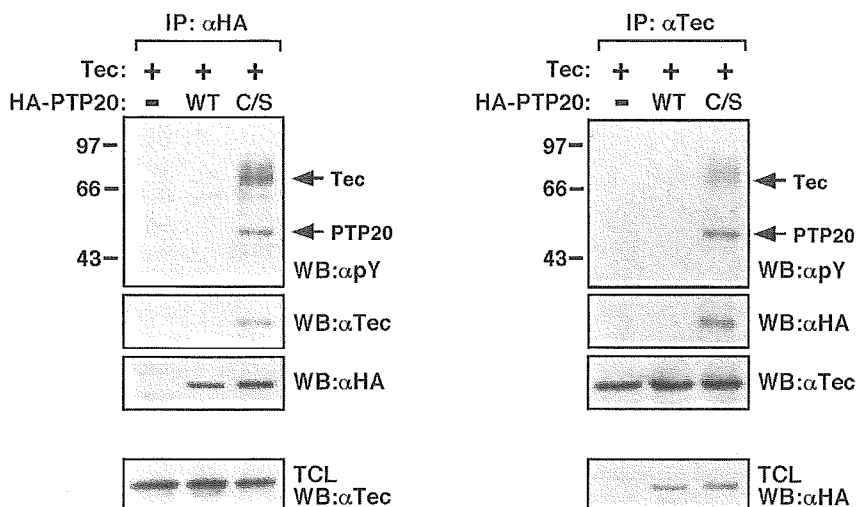
minal non-catalytic region of PTP20 are involved in not only binding to the Tec SH2 domain but also in the phosphorylation and subsequent activation of Tec.

We asked whether the C-terminal non-catalytic region of PTP20 was enough for phosphorylation and activation of Tec. To this end, PTP20 deletion mutants lacking either an N-terminal catalytic or a C-terminal non-catalytic segment were made, but the resultant constructs could not be expressed in COS7 cells, although comparable amounts of transcripts were detected (data not shown). To solve this problem, the N-terminal PTP domain and the C-terminal PEST domain were inserted into pEBG vector and were expressed as GST fusion proteins in COS7 cells. These pEBG plasmids encoding the PTP domain and full length of PTP20 C/S mutant and the PEST domain of PTP20 were co-transfected into COS7 together with Tec. Anti-phosphotyrosine blotting documented that Tec was highly tyrosine-phosphorylated with the full-length but not the PTP domain of the PTP20 C/S mutant (Fig. 6, *panel A*), supporting previous data shown in Fig. 5, where the C-terminal part of PTP20 was essential for tyrosine phosphorylation of Tec. Interestingly, the presence of the PEST domain of PTP20 caused tyrosine phosphorylation of PTP20, but the extent was lower than in the presence of the full-length PTP20 C/S mutant. Equivalent expression of each construct was confirmed by Western blotting with anti-Tec and anti-GST antibodies. To further examine the involvement of the PEST domain, lysates were precipitated with GSH-Sepharose beads followed by immunoblotting with anti-phosphotyrosine antibody. A phosphorylated 74-kDa band, which was shown to be Tec by immunoblotting, was co-precipitated with full-length PTP20 C/S mutant, whereas the PTP domain alone could not capture Tec (Fig. 6, *panel B*). A faint tyrosine-phosphorylated band with the same mobility of 74 kDa that co-precipitated with the PEST domain appeared to be Tec but could not be detected by our anti-Tec antibody presumably due to sensitivity. These results suggest that the PEST domain of PTP20 is necessary but not sufficient for not only hyperphosphorylation and activation of, but also association with Tec.

Negative Regulatory Roles of PTP20 in BCR Signaling—All the experiments documented above were conducted in transfected COS7 cells. To demonstrate a physiological relevance of the PTP20-Tec interaction, evidence of such an association in non-transfected cells was required. To this end we selected human Ramos immature B cells, because it has been reported that they express relatively high amounts of endogenous Tec (21). As shown above, interaction of PTP20 with Tec is mediated by tyrosine phosphorylation of PTP20, and PTP20 has autodephosphorylation activity, implying that it would be dif-

ficult to detect a phosphotyrosine-dependent interaction of PTP20 with other molecules including Tec endogenously. To overcome this experimental difficulty, protein-tyrosine phosphorylation was induced in Ramos cells by treatment with pervanadate (POV). Cells were starved for 16 h in serum-free medium and then either left unstimulated or treated with 0.1 mM POV for 30 min and lysed. Cell lysates were immunoprecipitated with either anti-phosphotyrosine antibody or anti-Tec antibody. Our PTP20-specific antibody could not be used due to its inability in immunoprecipitation experiments. In anti-phosphotyrosine immunoprecipitates, specific bands with 74 and 50 kDa corresponding to human Tec and PTP20 were detected only upon POV treatment (Fig. 7). A tyrosine-phosphorylated band with 50 kDa in the anti-Tec immunoprecipitates was readily detected by the anti-PTP20 antibody but only when cells received POV pretreatment (Fig. 7). These results indicate that endogenous Tec and PTP20 interact with each other in a phosphotyrosine-dependent manner in Ramos B cells.

Although upstream regulators such as cytokine receptors, lymphocyte surface antigens, G protein-coupled receptors, receptor type PTKs, or integrins for Tec in blood cells including Ramos B cells have been relatively well investigated (13, 20, 22–26), only limited information regarding downstream regulators of Tec has been available so far. If the data obtained in transfected COS7 cells are true, PTP20 would be thought to play a negative regulatory role in Tec-mediated signaling. To examine this, either the PTP20 WT, the inactive C/S mutant, or another form of catalytically inactive mutant D/A was transiently co-transfected with the pfos/luc reporter plasmid into Ramos cells, because the promoter of the c-*fos* proto-oncogene is activated in response to BCR cross-linking in the cells. Cells were either left unstimulated or treated with anti-human IgM F(ab')₂ fragments for 5 h. Cell lysates were assayed for luciferase activity. BCR cross-linking induced a marked activation of the c-*fos* promoter (Fig. 8). Expression of PTP20 WT totally inhibited BCR-induced activation of the c-*fos* promoter as well as its basal activity, whereas only about 20% inhibition of the promoter activation was observed in the co-expression of catalytically inactive forms of PTP20, strongly indicating that PTP20 is a negative regulator of BCR-Tec-c-*fos* signaling.

Tyrosine Phosphorylation of PTP20 by Tec Modulates Its Catalytic Activity against Tec as Well as Itself—We demonstrated that specific tyrosine residues Tyr-281, Tyr-303, Tyr-354, and Tyr-381 of PTP20 could be phosphorylated by Tec and served as Tec binding sites (Fig. 5). To further investigate physiological relevance of PTP20 tyrosine phosphorylation, substitution of the tyrosine residues with phenylalanine in PTP20 WT was performed. The YF mutants of HA-PTP20 WT